

## General Disclaimer

### One or more of the Following Statements may affect this Document

- This document has been reproduced from the best copy furnished by the organizational source. It is being released in the interest of making available as much information as possible.
- This document may contain data, which exceeds the sheet parameters. It was furnished in this condition by the organizational source and is the best copy available.
- This document may contain tone-on-tone or color graphs, charts and/or pictures, which have been reproduced in black and white.
- This document is paginated as submitted by the original source.
- Portions of this document are not fully legible due to the historical nature of some of the material. However, it is the best reproduction available from the original submission.

FINAL REPORT

to the

GEORGE C. MARSHALL SPACE FLIGHT CENTER

NATIONAL AERONAUTICS AND SPACE ADMINISTRATION

on

ANALYSIS OF THE CAPABILITY AND LIMITATIONS OF RELATIVISTIC

GRAVITY MEASUREMENTS USING RADIO ASTRONOMY METHODS

submitted by the

Department of Earth and Planetary Sciences

Massachusetts Institute of Technology

Cambridge, Massachusetts 02139

Control No.: 4330

Contract No.: NAS8-30301

Period of Performance: 1 October 1973 - 30 June 1975

Principal Investigators:

---

Irwin I. Shapiro  
Prof. of Geophysics &  
Physics  
Soc. Sec. No. [REDACTED]  
Tel. 617-253-5734

---

Charles C. Counselman III  
Assoc. Prof. of Planetary  
Science  
Soc. Sec. No. [REDACTED]  
Tel. 617-253-7902



30 June 1975

N75-29962  
Unclas  
33024  
G3/89  
(NASA-CR-120687) ANALYSIS OF THE CAPABILITY AND LIMITATIONS OF RELATIVISTIC GRAVITY MEASUREMENTS USING RADIO ASTRONOMY METHODS Final Report, 1 Oct. 1973 - 30 Jun. 1975 (Massachusetts Inst. of Tech.) 146 p HC

This report was prepared by the Department of Earth and Planetary Sciences of the Massachusetts Institute of Technology under Contract No. 4330/NAS 8-30301, "Analysis of the Capability and Limitations of Relativistic Gravity Measurements Using Radio Astronomy Methods", for the George C. Marshall Space Flight Center of the National Aeronautics and Space Administration.

Table of Contents

	<u>Page</u>
Abstract	6
Forward	7
Part I	8
Radar Tests of Relativity	8
I.    Introduction	8
II.   Relativistic Effects on Radar Measurements	10
1.  Parameterization of the Schwarzschild Metric	10
2.  Retardation of Signal Propagation	12
3.  Deflection of Signals	13
4.  Advance of Planetary Perihelia	13
5.  Possible Time Variation of the Gravi- tational Constant	14
6.  Possible Violation of the Principle of Equivalence	18
7.  Gravitational "Redshift"	21
8.  Lense-Thirring Effect	22
III.  Effects Corrupting Relativity Tests	24
1.  Earth Rotation	24
2.  Site Locations	25

III. (continued)	Page
3. Propagation Medium	27
i. Atmosphere and Ionosphere of the Earth	28
ii. Atmosphere and Ionosphere of the Target Planet	30
iii. Interplanetary Plasma and Solar Corona	32
4. Gravitational Perturbations	42
i. Galaxy	42
ii. Neighboring Stars	43
iii. Sun	43
(1) Mass Distribution	44
(2) Mass Changes	47
(3) Tides	50
iv. Planets	50
(1) Orbits	51
(2) Masses	52
(3) Spin-Orbit Coupling	54
v. Asteroids	55
vi. Satellites	58
(1) The Moon	59
(2) Phobos and Deimos	59
(3) Satellites of Outer Planets	61
5. Non-Gravitational Perturbations	61
i. Electromagnetic Radiation	62
ii. Solar Wind	66

	Page
III. 5. (continued)	
iii. Particulate Matter	67
6. Planetary Topography	69
i. Methods of Measurement	69
(1) Topography at the Subradar Point	70
(2) Topography Along the Doppler Equator	73
(3) Topography Over the Visible Hemisphere	79
ii. Methods of Analysis	82
IV. Current Status and Prospects for Radar Tests of Relativity	89
1. Retardation of Signal Propagation	90
2. Advance of Planetary Perihelia	96
3. Variation of the Gravitational Constant	105
4. Principle of Equivalence	107
References for Part I	110
 Part II	
Radio-Interferometric Measurement of the Solar Gravitational Deflection of Radio Waves	113
I. Introduction	113
II. Observations	118
III. Analysis	124
IV. Result and Estimate of Uncertainty	127
V. Future Experiments	136
References for Part II	146

The uses of radar observations of planets and very-long-baseline radio interferometric observations of extragalactic objects to test theories of gravitation are described in detail with special emphasis on sources of error. The accuracy achievable in these tests with data already obtained, can be summarized in terms of standard notation as follows:

Retardation of signal propagation (radar):	$\sigma\left(\frac{1+\gamma}{2}\right)$	$\approx 0.04$
Deflection of radio waves (interferometry):	$\sigma\left(\frac{1+\gamma}{2}\right)$	$\approx 0.03$
Advance of planetary perihelia (radar):	$\sigma\left(\frac{2+2\gamma-\beta}{3}\right)$	$\approx 0.04$
Gravitational quadrupole moment of sun (radar):	$\sigma(J_2)$	$\approx 1.5 \times 10^{-5}$
Time variation of gravitational constant (radar):	$\sigma\left(\frac{\dot{G}}{G}\right)$	$\approx 10^{-10} \text{ yr}^{-1}$

The analyses completed to date have yielded no significant disagreement with the predictions of general relativity. If radar and radio observations are pursued in the manners herein proposed, the uncertainties in these experiments could be reliably reduced to

$$\begin{aligned}\sigma\left(\frac{1+\gamma}{2}\right) &\leq 0.003 \text{ (radar)} \\ \sigma\left(\frac{1+\gamma}{2}\right) &\leq 0.003 \text{ (radio interferometry)} \\ \sigma\left(\frac{2+2\gamma-\beta}{3}\right) &\leq 0.01 \text{ (radar)} \\ \sigma(J_2) &\leq 3 \times 10^{-6} \text{ (radar)} \\ \sigma\left(\frac{\dot{G}}{G}\right) &\leq 2 \times 10^{-11} \text{ yr}^{-1} \text{ (radar)}\end{aligned}$$

by the early 1980's. In addition, a significant radar test could be made in this time period of the Principle of Equivalence, in regard to the relative contributions of gravitational binding energy to inertial and gravitational masses. Combination of radar and spacecraft ranging data would yield improvements in almost all of these tests.

Foreward

We are concerned in this report with the evaluation of the state of the art in testing theories of gravitation using two radio-astronomy methods: radar time-delay measurements and very-long-baseline interferometry (VLBI) ray-deflection measurements. For convenience, we have therefore divided the report into two parts. In Part I we discuss the radar method, but give relatively little emphasis to a description of the basic measurement technique since it is already well documented in the literature. In Part II, by contrast, we describe in some detail the VLBI technique as applied to testing theories of gravitation, since this method is newer and consequently less well known than the radar method. In both parts of the report, we conclude with a consideration of possible improvements in the accuracy of the relevant tests of gravitation.



Part I

Radar Tests of Relativity

I. Introduction

Radar tests of the theory of general relativity, or, more generally, of theories of gravitation have been in progress for more than a decade and several useful results have already been obtained. Reviews of this work, containing references to the original publications, can be found in several articles (Shapiro, 1972 and 1973).

Interplanetary radar measurements which form the basis of these tests primarily concern the round-trip time delays and the Doppler shifts of the echoes. The time delays have fractional uncertainties far less than those for the Doppler shifts and are the principal measurements underlying the tests of theories of gravitation. Relativistic effects, on general grounds, can be expected to appear when the fractional uncertainties in the delay measurements dip below  $(v^2/c^2)$   $\sim 10^{-8}$ , with  $v$  a typical orbital velocity for a planet, or below about  $10^{-7}$  for ray paths that nearly graze the solar limb.

Radar system sensitivity has been increasing, on average, by about 5.5 db/yr since 1946 and, at present, fractional delay-measurement uncertainties for some favorable planetary con-

figurations are as low as 2 parts in  $10^{10}$ . On the horizon is the upgraded Arecibo radar facility which, after it begins routine operation in mid 1975, should extend such accuracies to most configurations of the inner planets as well as increasing the accuracies for certain configurations. The limitations in these latter circumstances will be set by considerations other than the basic radar system sensitivity.

The above statements indicate the general feasibility of performing precision tests of theories of gravitation with radar measurements. However, one must be cautious: In addition to information about relativistic effects on the signal propagation and on the motion of the observed body and the observing platform, there exist other nonrelativistic influences on the delays. These can be either of a random, unpredictable nature or of a type that has a signature highly correlated with the sought-for relativistic effects. In both cases, the net result is to degrade the accuracy of the tests of gravitation theories and, therefore, such other influences will be considered "corrupting" for the purposes of this report.

We divide the remainder of this part into three main sections. In the first, we discuss the various radar tests that appear feasible and include approximate magnitudes of the relativistic effects involved. In the second, we consider in a rather encyclopedic fashion, effects that might corrupt the tests and the means for the elimination or reduction of their adverse influences. The final section is devoted to a brief

summary of the present status of the relativity tests and an indication of the possible improvements that could be anticipated in the next decade.

## II. Relativistic Effects on Radar Measurements

We discuss relativistic effects primarily, but not exclusively, in the context of the Schwarzschild solution. With one exception, we consider the relativistic effects of the sun to stem from a non-rotating, spherically-symmetric mass distribution. The relativistic effects stemming from the non-zero masses of the planets can be ignored. This last conclusion follows from the formal solution to the post-Newtonian (weak field) equations for the solar system, derived many times by many authors over the past half century (see, for examples, Tausner, 1966 and Weinberg, 1972).

Our direct concern is with the relativistic effects caused by the sun on the propagation of radio waves and on the motions of the inner planets, Mercury through Mars. The orbits and masses of the outer planets may be assumed known in that the uncertainties in these quantities, determined separately from the direct observations of the outer planets, cause uncertainties in our interpretation of the inner-planet observations that with few exceptions (see Section III) are too small to affect the relativity tests presently of interest.

### 1. Parameterization of the Schwarzschild Metric

Eddington (1960), and later Robertson (1962), sought

to generalize the space-time metric that represents the (exterior) Schwarzschild solution for the sun partly to formalize comparisons with experimental results. They chose a particular parameterization which is analogous to the parameterized multipole expansion often used for an unknown charge distribution. For the Schwarzschild solution expressed in so-called isotropic coordinates, the Eddington-Robertson form of the metric is

$$ds^2 = [1 - 2\alpha \left(\frac{r_0}{r}\right) + 2\beta \left(\frac{r_0}{r}\right)^2 + \dots] c^2 dt^2 - [1 + 2\gamma \left(\frac{r_0}{r}\right) + \dots] [dx^2 + dy^2 + dz^2], \quad (2.1)$$

where  $ds$  represents the element of arclength in the four-dimensional space-time;  $dx$ ,  $dy$ , and  $dz$  are the differentials of the space coordinates;  $dt$  is the differential of time;  $c$  is the speed of light; and  $\alpha$ ,  $\beta$ , and  $\gamma$  are the parameters.\*

A more complete, and very elegant, parameterization of metric theories of gravitation in the post-Newtonian approximation has been developed over the past few years by Nordtvedt, Thorne, and Will (see Will, 1973 for a thorough discussion). However, the parameterization given in Equation (2.1)

---

\* In view of the excellent agreement of planetary orbits with Newtonian theory, for example, one can conclude without further ado that  $\alpha$  is equal to unity.

will, for the most part, be adequate for our purposes. Since the parameters  $\gamma$  and  $\beta$  in this parameterization affect both signal propagation and planetary motions, we will discuss each effect in turn.

## 2. Retardation of Signal Propagation

The Eddington-Robertson metric, as does the Schwarzschild solution itself, predicts a retardation of, or delay in, signal propagation when rays pass near a massive body. In particular, as was first shown a decade ago (Shapiro, 1964), the "excess" delay,  $\Delta\tau_r$  is predicted to obey:

$$\Delta\tau_r = \frac{2(1+\gamma)r_o}{c} \ln \left( \frac{r_e + r_p + R}{r_e + r_p - R} \right), \quad (2.2)$$

where  $r_o \equiv (GM_\odot/c^2) \approx 1.5$  km is the gravitational radius of the sun;  $G$  the gravitational constant;  $M_\odot$  the sun's mass;  $c$  the speed of light;  $r_e$  the heliocentric distance of the earth;  $r_p$  the heliocentric distance of the target planet; and  $R$  the earth-planet distance. The maximum predicted effect (with  $\gamma=1$ ) is approximately 250  $\mu$ sec for a signal path that grazes the solar limb. But, as intimated above, the "observable" effect is, in effect, reduced by other nonrelativistic influences on the round-trip time delays.

Note that the expression (2.2), accurate to first order in  $r_0$ , is independent of  $\beta$ . A dependence of the time delay on  $\beta$  enters to this order only through the relativistic effects on planetary orbits. The direct effects of solar gravity on the time delays are sensitive only to  $\gamma$  (Shapiro, 1966).

### 3. Deflection of Signals

Interferometric radar observations of a planet can be employed to measure the predicted gravitational deflection,  $\eta$ , of the radar signals by the sun (Shapiro, 1967):

$$\eta = \frac{(1+\gamma)r_0}{r_e} \tan\left(\frac{\theta}{2}\right), \quad (2.3)$$

where  $\theta$  is the planet-sun-earth angle. Because of the finite planet-earth separation, the maximum deflection of 1.75 arcsec ( $\gamma=1$ ) is not attained. Thus, for Venus the target planet and with the signals grazing the limb of the sun,  $\eta \approx 0.73$  arcsec ( $\gamma=1$ ). This experiment has never been performed because higher accuracy appears to be obtainable from the corresponding radio interferometric observations of cosmic radio sources, as discussed in Part II of this report.

### 4. Advance of Planetary Perihelia

As has been known since the inception of the theory over a half-century ago, general relativity and its Edington-Robertson generalization predict a secular advance of planetary perihelia, given by

$$\Delta\omega \approx \left(\frac{2+2\gamma-\beta}{3}\right) \frac{6\pi r_0}{p} \text{ rad/rev}, \quad (2.4)$$

where  $p$  is the semilatus rectum of the orbit. Clearly the advance is sensitive to both  $\gamma$  and  $\beta$  with the sensitivity to  $\gamma$  being twofold greater. The effect of this "excess" ad-

vance on the measurement of time delays is bounded, very crudely, for radar observations of Mercury by

$$\Delta\tau_{adv} < 2ea\Delta\omega \approx 160 \mu\text{sec/yr} \quad (2.5)$$

where  $e$  is the eccentricity and  $a$  the semimajor axis of Mercury's orbit. The value for  $\Delta\omega$  is given by Equation (2.4) but scaled to the total advance per year, about 0.4 arcsec; both  $\gamma$  and  $\beta$  were set to unity in accord with the predictions of general relativity. The factor of two in Equation (2.5) accounts for the round-trip aspect of the delays.

There are other, short-period relativistic terms in the description of planetary orbital motions. These, for Mercury, have amplitudes of up to about 40  $\mu\text{sec}$ . But their "observability" is doubtless much diminished by correlations with the orbital elements, or initial conditions, of planetary motion which perforce must also be estimated from the same time-delay data since no other data are of sufficient accuracy. A similar comment applies to the relativistic deviations predicted from Kepler's third law for a suite of planetary orbits. As far as we are aware, no careful study has yet been carried out to isolate, in an operational manner, the contributions each of these orbital effects could make to the determinations of  $\gamma$  and  $\beta$ , and, in particular, to their separation from the dynamical effects of the solar gravitational quadrupole moment (see Section III.iii.1). In all covariance studies so far carried out all such effects are lumped together.

##### 5. Possible Time Variation of the Gravitational Constant

According to both Newtonian precepts and Einstein's theory of general relativity (and its Eddington-Robertson generalization), the constant of gravitation is indeed a

universal constant. On the basis of other theories of gravitation, such as the Brans-Dicke scalar-tensor theory (see, for discussions, Weinberg, 1972 and Misner, Thorne, and Wheeler, 1973), the constant of gravitation should be weakening slowly with time as the universe expands. This weakening would be observable through measurements that depended on atomic constants. In other words, on the basis of such theories, a "gravitational" clock would appear to slow down as measured by an atomic clock. In particular, if the mean motion,  $\underline{n}$ , of a planet were measured with an atomic clock, it would be predicted to decrease in a secular fashion according to the formula

$$\frac{\dot{\underline{n}}}{\underline{n}} = 2 \frac{\dot{G}}{G}, \quad (2.6)$$

where a dot indicates differentiation with respect to time. This effect would be the more noticeable the larger the mean motion. Thus, of the planets, Mercury is the most useful gravitational clock for the detection of any such time variation of G. The moon, although it has approximately a threefold higher mean motion than Mercury, suffers from being too close to the earth with the consequence that tidal interactions are strong and difficult to separate from the effects of any possible change in G.

A change in G causes a change in the earth-planet time delay, due to a change,  $\Delta L$ , in the mean longitude of the planet, bounded by (Shapiro et al., 1971a):



$$\Delta\tau_{\dot{G}} \leq 2a\Delta L = 2an\frac{\dot{G}}{G}T^2, \quad (2.7)$$

since

$$\Delta L = \int_0^T \dot{n} t dt = \frac{1}{2} \dot{n} T^2 = n \frac{\dot{G}}{G} T^2. \quad (2.8)$$

Here  $T$  is the interval over which the delay observations have extended. For Mercury, with  $(\dot{G}/G) \approx 1 \times 10^{-10}$  per year, we obtain

$$\Delta\tau_{\dot{G}} \leq T^2 \mu\text{sec} \quad (2.9)$$

with  $T$  in years. Thus  $\Delta\tau_{\dot{G}} \leq 25 \mu\text{sec}$  after 5 years.

Note that there have been attempts to estimate  $\dot{G}/G$  from studies of lunar motion, notwithstanding the difficult problems posed by tidal interactions (see, for example, Slade 1971). In the most recent attempt, Van Flandern (1975) claims to have detected a significant change:  $(\dot{G}/G) = (-7.5 \pm 2.7) \times 10^{-11}$  per year, based partly on an analysis of 18 years of lunar occultation data which allow him to estimate the acceleration in mean longitude shown in Equation (2.8). However, for the moon, in 18 years, the change in  $\Delta L$  would be only about 0.4 arcsec for this value of  $(\dot{G}/G)$ .

Again we must emphasize that the whole effect here is by no means "observable". First, we note that a parabola, such as given by Equation (2.9), can be fit by a straight line with the deviation nowhere exceeding one eighth of the total "growth" of the parabola. Thus, unless measurement errors were under, say, 3  $\mu$ sec, we would have difficulty, based on only 5 years of earth-Mercury time-delay observations, in distinguishing a change in  $G$  of 1 part in  $10^{10}$  per year from a modification in our estimate of Mercury's mean motion. [Recall that the slope of the best-fit straight line to the parabola of Equation (2.9) would be interpreted, in this oversimplified analysis, as a correction to the estimate of Mercury's mean motion.] Second, we mention that the actual estimate of  $\dot{G}$  would involve a simultaneous solution for all relevant parameters with the consequence that the "observable" effect would actually be reduced by an amount even larger than the factor of eight reduction entailed by the effective "masking" of a parabola that can be accomplished by a straight line.

The above arguments apply as well to the interpretation of changes in the moon's mean longitude that might be due to a variation in the gravitational constant (see Section IV. 4). In view of these and other aspects of the analysis, we consider that Van Flandern has underestimated the uncertainty of his result which, in our opinion, is not significantly different from zero.

Finally, we remark that in certain theories of gravitation, spatial variations of the gravitational constant are predicted. It does not appear feasible to use interplanetary radar measurements to detect or to set useful bounds on such possible variations. However, a detailed analysis of this problem has not been carried out.

#### 6. Possible Violation of the Principle of Equivalence

A cornerstone of Einstein's theory of general relativity is the Principle of Equivalence. In its so-called weak form, this principle states that the ratio of the gravitational to the inertial mass of a body is independent of its composition and size. This principle has been tested in the laboratory with ever-increasing accuracy over the past

three centuries, starting with Newton's demonstration which established the validity of the principle to about 1 part in  $10^3$ . The most accurate test was carried out by Braginski and Panov (1971) who concluded that the principle held to at least a few parts in  $10^{12}$ . Although these laboratory tests demonstrate, for example, that the binding energy of the electrons in atoms and of the nucleons in the nucleus contribute equally to inertial and gravitational masses, these tests fail utterly to shed light on whether the gravitational binding energy contributes equally to inertial and gravitational masses: For a laboratory-sized object, the gravitational binding energy constitutes no more than about 1 part in  $10^{23}$  of the total mass, far below the sensitivity of the laboratory tests. Since this fractional contribution varies approximately as the square of the body's dimension, one needs planetary-sized bodies to perform a meaningful test for the gravitational binding energy. Let us define the ratio of the gravitational to inertial mass such that

$$\frac{M_G}{M_I} - 1 = \Delta, \tag{2.10}$$

where  $\Delta$ , by assumption, accounts for any possible deviation from the Principle of Equivalence due to an unequal contribution of the gravitational binding energy to  $M_G$  and  $M_I$ . For the sun, then, we'd expect  $\Delta$  to be bounded by  $O(10^{-5})$  and,

for Jupiter and the earth, by about  $O(10^{-8})$  and  $O(10^{-9})$ , respectively.

A two-body orbiting system is not useful for a test of the principle of equivalence since the implied violation of Kepler's third law, which relates the period and semi-major axis of such a system, is unobservable due to the lack of an independent determination of the relevant masses. However, three or more mutually orbiting bodies do provide a possible test.

Renewed interest in such a test was kindled by Nordtvedt (1968) who showed that this weak Principle of Equivalence was violated for massive bodies in the Brans-Dicke theory, a consequence not previously recognized. More specifically, Nordtvedt showed that a violation would introduce a variation in the radial separation of two of the bodies (say, the earth and the moon) of a three-body system (say, the earth-moon-sun system) proportional to:

$$4\beta - \gamma - 3 - \alpha_1 + \frac{2}{3}\alpha_2 - \frac{2}{3}\zeta_1 - \frac{1}{3}\zeta_2. \quad (2.11)$$

We omit the exact definitions of the parameters  $\alpha_1$ ,  $\alpha_2$ ,  $\zeta_1$ , and  $\zeta_2$ , as they are not germane to our discussion; see Will (1973) for a detailed description. We remark here only that, for general relativity, the terms

on the right side of Equation (2.11) sum to zero whereas this sum does not vanish under the Brans-Dicke theory.

Considerable attention has been given to the possible detection of a nonzero value for  $\Delta$  from analysis of lunar laser observations, the relevant three-body system being the earth, the moon, and the sun. In the radar context, we have examined the possibility for detection of a violation with respect to the four-body system: earth-Mars-Jupiter-sun. In particular, we have considered using earth-Mars time-delay observations; a very detailed, but still incomplete, study of this possibility was made at M.I.T. by Sherman (1973). Similar observations of Venus, especially, and of Mercury will also be very efficacious in strengthening this test.

For a violation of the weak Principle of Equivalence of the order of the ratio of the gravitational self energy to the total energy of a body, it can be shown that the effect on the earth-Mars time-delay measurements, for example, would be of the order of 10  $\mu$ sec (Sherman, 1973). But masking will reduce its observability. We note that the effect of a nonzero  $\Delta$  will be in large part periodic, with periods approximately those of the earth and target planet.

#### 7. Gravitational "Redshift"

The gravitational "redshift", the effect of the local gravitational potential on the apparent frequency of a light wave which causes a spectral line generated at the sun to appear red-shifted when observed on earth, does not seem amenable to direct measurement in interplanetary radar experiments. However, the concomitant predicted effect on clock rates is susceptible of detection. Because

of the eccentricity of the earth's orbit, an atomic clock on earth, relative to that of a distant observer, is predicted to undergo yearly variations of amplitude about 1.5 msec. This effect, relative to the situation in its absence, causes the time-delay measurements to be referred to a different epoch. If the reference epoch is in error, however, the calculated delay -- in the absence of any other errors or inexact parameter values -- would disagree with the observed delay by the product of the epoch error and the time rate of change of the delay. For interplanetary observations, the delay rate can be as high as  $2(v/c) \approx 200 \mu\text{sec}/\text{sec}$ . Hence an epoch error of 1.5 msec would manifest itself in delay residuals of maximum magnitude of about  $0.3 \mu\text{sec}$ . Such an effect is too small to be reliably detected with useful accuracy at present, especially when masking is considered, and so will not be discussed further in this report.

#### 8. Lense-Thirring Effect

Lense and Thirring (1918) predicted on the basis of the then new theory of general relativity that a rotating mass tended to rotate a "nearby" inertial frame in the same direction. Incorporation of the sun's rotation, therefore, produces a modification of the Schwarzschild solution which has consequences for both the propagation of radio signals and the orbits of planets. In addition, the spin axis of these orbiting bodies would undergo additional precession due to the Lense-Thirring effect. None of these consequences

of the theory of general relativity, or its generalization, has so far been observed.

A program undertaken at Stanford University, with NASA sponsorship, has for over a decade been concerned with the development of a superconducting gyroscope to orbit the earth to detect the so-called "geodesic precession" and the much smaller Lense-Thirring precession which, in the terrestrial context, amounts to only some hundredths of an arcsecond per year (see Misner, Thorne, and Wheeler, 1973, and references cited therein). Any actual measurements are still some years in the future.

A preliminary study was undertaken at M.I.T. (Miller, 1971) to ascertain the possible observability of the Lense-Thirring effect on interplanetary time-delay measurements. The results, as expected, were not encouraging. The effect on the earth-Mercury time-delays, due to the effect on the orbit of Mercury, is of the order of 1 nsec per orbital revolution. Worse, the lack of precise knowledge of the sun's angular momentum vector makes the effect even more difficult to detect. We therefore end discussion of this effect for the purposes of this report.



### III. Effects Corrupting Relativity Tests

Here we discuss the various effects on the radar time-delay measurements that, for the purpose of testing theories of gravitation, may be considered as corrupting influences, or as "noise". In contrast to the discussion of relativistic effects, we treat these corrupting effects in approximately the reverse order of their magnitude, reserving the most serious -- planetary topography -- for last.

#### 1. Earth Rotation

Since all observations are made from the earth's surface, the motion about the center of mass influences the time-delay observations. The earth's deviations from solid-body rotation with a constant angular velocity about a fixed axis in inertial space are conventionally described by the precession, nutation, polar motion, variations in UT.1, and solid-body tides of the earth. These deviations are currently known with sufficient accuracy that, for purposes of analyzing a decade of interplanetary radar measurements, the uncertainty in the position of a point on the earth's surface with respect to an inertial frame is of the order of 5 meters or approximately 0.03  $\mu$ sec in equivalent two-way light time.

Such an uncertainty is of no consequence for the interpretation of existing radar data and will pose no severe problem for the interpretation of data to be obtained in the future. However, with the development of very-long-baseline interferometry (VLBI), the uncertainty in the changes in the earth's position with respect to an inertial frame formed by distant extragalactic radio sources will be reduced over the next few years to the decimeter level ( $\lesssim 0.002 \mu\text{sec}$  in equivalent light time) and so will be an utterly negligible source of corruption for radar tests of relativity.

## 2. Site Locations

In addition to the determination of the earth's orientation in inertial space, one must also determine the location of the radar site on the earth. For some of the delay measurements already made, as well as for most of the future measurements, conventional geodetic surveys do not provide sufficient accuracy. Of course, one can add the site coordinates to the parameter list, as we have in fact done, and estimate these along with the other solar-system parameters of interest; the correlations with the estimates of the parameters describing the relativistic effects are very low. If for no other reason than as an independent check, however, it is desirable to determine the site locations

by other means. The VLBI technique provides such a means; moreover, through its use, the radar sites can be located with respect to the same inertial frame in which the earth's orientation is described. We have already conducted a series of VLBI experiments between Goldstone and Haystack (Shapiro et al., 1974) which serves to establish their relative location to within 1 m\*. We have also submitted a proposal to do a similar, but for technical reasons somewhat less accurate, VLBI experiment between Haystack and Arecibo. The results will allow the relative locations of all three sites to be determined to within a few meters which should provide a powerful check on the estimates of the site locations made from an analysis of the radar data from these three sites.

We should also note that through VLBI the orientation of the planetary system itself can be determined with respect to the same inertial frame used to specify the earth's

---

\*From VLBI observations of extragalactic sources, the baseline of the interferometer is determined, with respect to the inertial frame formed by these sources, to within a parallel displacement. Lack of parallax leads to this freedom in the specification.

orientation (Counselman et al., 1972)\*. The method proposed to accomplish this determination involves differential measurements of extragalactic radio sources and transmitters aboard spacecraft that are either flying by, orbiting, or landed on another planet. By observing simultaneously, or near simultaneously, with a very-long-baseline interferometer, both the signals from the spacecraft and those from an extragalactic radio source, when the latter is nearly in the same direction from the earth as the planet, high accuracy can be obtained. Recently our VLBI group (see Part II) has used this technique to determine the angular separation between two extragalactic radio sources with an uncertainty of only about 0".001; the same accuracy could be achievable in the determination of the orientation of the planets with respect to such extragalactic sources. The main problem is the lack of suitable opportunities.

### 3. Propagation Medium

The medium through which the radar signals pass obviously affects the values of the measured time delays. For purposes of discussion, we separate the medium into

---

\* Because of the rather weak dynamical coupling between the earth's spin angular momentum vector and the angular momentum vector of the planetary system, the determination of the orientation of one of these vectors with respect to a given frame doesn't of itself determine the orientation of the other with respect to that frame.

three parts: the earth's atmosphere and ionosphere, the target planet's atmosphere and ionosphere, and the interplanetary plasma and solar corona.

i. Atmosphere and Ionosphere of the Earth

The neutral atmosphere has an electrical path length of slightly under 3 meters in the zenith direction; this length increases as the secant of the zenith angle (co-secant of the elevation angle). The lowest elevation angles usually employed in interplanetary radar experiments are about  $6^\circ$  for which the two-way effect on delay is about  $0.2 \mu\text{sec}$ . Models for the neutral atmosphere in current use are accurate to about 10% in their ability to predict the electrical path length at microwave frequencies. (This rather large uncertainty is due primarily to the difficulty in modeling the very variable contribution of the atmospheric water vapor.) Thus, the uncertainty in the theoretical calculation of the contribution of the neutral atmosphere to the values of the time-delay measurements is never greater than  $0.02 \mu\text{sec}$ . Moreover, for the Arecibo radar facility, the elevation angle can never drop below about  $70^\circ$ , implying a limit on our uncertainty in the atmosphere's contribution of under  $0.002 \mu\text{sec}$  which will not be of any consequence.

The effect of the earth's ionosphere is, of course, frequency dependent. For the radar frequency of 7840 MHz used

at the Haystack Observatory, the effect on the time-delay values has always been negligible compared to the measurement accuracy. At the 2388 MHz radar frequency used at the Goldstone Tracking Station, the contribution of the ionosphere to the time delay during the day is of the same order as the contribution of the neutral atmosphere for high elevation angles; the ionospheric contribution, however, increases far less rapidly as the elevation drops below about 30°. Thus, the maximum contribution of the ionosphere to the delays measured at Goldstone is about 0.06  $\mu$ sec and is small compared to their current delay measurement accuracy.

At Arecibo, the currently used radar frequency is 430 MHz for which the maximum contribution of the ionosphere to the delay measurements is about 0.6  $\mu$ sec (recall the 70° lower limit on elevation angles). This contribution can not at present be modelled with an uncertainty any smaller than about 30%, leaving the unmodelled part of the ionosphere contribution to the delay at about 0.2  $\mu$ sec for the daytime observations of Mercury and Venus. This uncertainty is almost as large as that accompanying the most accurate measurements currently being made in observations of these two planets at the Arecibo Observatory. For the past observations of Mars near opposition, the signal passed through the

night-time ionosphere for which the ionospheric effect on delay is tenfold smaller, yielding a maximum uncertainty in the ionosphere contribution of about 0.02  $\mu$ sec which is negligible.

By the end of this year, before the next opposition of Mars, the upgrading of the Arecibo radar will be completed; subsequent planetary observations will be made at a radar frequency of 2380 MHz with a consequent 30-fold reduction in the influence of the ionosphere.

ii. Atmosphere and Ionosphere of the Target Planet

Of the inner planets, only Venus has a significant neutral atmosphere from the point of view of affecting radar time-delay measurements. For observations of the delay to the subradar point\*, only normal incidence is involved. Still, the incremental two-way delay introduced by Venus' neutral atmosphere is nearly 2  $\mu$ sec, virtually

---

\*The subradar point on a planet's surface is at the intersection there of the line drawn from the radar site to the planet's center of mass.

independent of the radar frequency\*. Despite its relative enormity, this effect is not as devastating as it seems. Our only concern, in regard to relativity tests, is with the spatial or temporal changes in the atmospheric delay. The predominant contributions to the delay come from the lower few scale heights and, primarily because of the very large inertia of the lower atmosphere, temporal and spatial variations are expected to be no larger than a few percent. Indicative of the validity of this expectation is the finding from earth-based radio interferometry (Sinclair et al., 1972) that the variation of the  $\approx 750^\circ\text{K}$  surface temperature over the disc of Venus is under  $15^\circ\text{K}$ . Variations in the contribution of the atmosphere to the radar time-delay measurements that are caused directly by the topographic variations with respect to an equipotential surface can be "lumped" in with the topography effects (see Section III. 6) and need cause no additional concerns. It is possible, in principle, to separate the atmospheric from the strictly

---

\*The absorption of the radar signal in Venus' atmosphere is, however, a strong function of frequency, increasing approximately as the square. Thus the two-way attenuation for observations of the subradar point is about 7 db at X-band, but virtually negligible at the S-band frequencies used at Goldstone and soon to be used at Arecibo.



topographic effects on delay as discussed by Shapiro et al. (1973), but the implementation of the technique proposed in that article is not needed for relativity-test purposes.

We note also that any error in modelling the (constant) delay introduced by Venus' atmosphere is of no concern; it is absorbed in the estimate from the radar data of the mean radius of Venus. Should an independent, and more accurate, estimate of the mean radius become available, as well as a better model for the atmospheric delay, then the comparison of that radius, as modified by the effect of the atmosphere, with the "radar" radius will allow another check to be made on the validity of the statistical filtering of the radar data.

Ionospheres on Venus and Mars have been measured using the radio-occultation technique (see, for example, Howard et al., 1974, and Kliore et al., 1972), but the integrated electron density in the zenith direction is, in each case, substantially smaller than that for the earth and poses no problem for the interpretation of either past or proposed radar observations of these planets.

iii. Interplanetary Plasma and Solar Corona

The sun emits, at high speed, charged particles that form the solar wind. This plasma, constituted primarily of electrons and protons, may for purposes of discussion be divided into two regimes: the

interplanetary plasma and the "inner" solar corona; the demarcation line is arbitrary but we place it here at about four or five solar radii since in general only signals passing outside that limit can yield useful interplanetary time-delay measurements. For signals that approach to about this distance from the sun, it becomes very difficult to obtain accurate delay measurements at S-band radio frequencies because the turbulence of the corona severely restricts the coherence time of the radar signal. For such distances, even at X-band frequencies the turbulence effects on the signals begin to affect the delay measurements adversely. At the 430 MHz radio frequency currently used by the Arecibo radar facility, useful measurements can not be made if the signal passes within about ten solar radii from the sun's center.

The above statements relate to average conditions of the solar wind. But the hallmark of the solar wind is its variability and, moreover, the unpredictability of this variability. It will be possible at times to make useful delay measurements at S-band for signals that approach within 4 radii of the sun; at other times, delay measurements will be thwarted for closest approach distances of 12 solar radii. Some examples of the enormous variability of the

turbulence of the solar wind are given in Part II of this report. Indications of the corresponding variability of the mean of the integrated electron density along paths passing near the sun are given in Figure 1 which is based on observations of the occultations of the Crab pulsar by the sun in 1973 (Weisberg et al., 1975; see also Counselman and Rankin, 1972).

Thus, for radar tests of relativity, one is restricted to signal paths that pass no closer to the sun than about four to five solar radii -- unless new radar facilities are built which utilize substantially higher radio frequencies. But what about the interplanetary plasma beyond? How does it affect the radar tests of relativity? Clearly the effect is greatest for the time-delay test (Section II. 2) which depends on the signal path passing close to the sun. To obtain a quantitative estimate of the corruption of this test due to the interplanetary plasma we can utilize an approximate relation for the charged particle density,  $N(r)$ , as a function of the distance,  $r$ , from the center of the sun:

$$N(r) \approx 5 \times 10^5 \left(\frac{R_{\odot}}{r}\right)^2 \text{ e1/cm}^3; \quad r \geq 5R_{\odot}, \quad (3.1)$$

where  $R_{\odot}$  is the radius of the sun. This formula yields the average values for the charged-particle density near  $10R_{\odot}$  but gives values somewhat too high near the earth's orbit ( $r \approx 200 R_{\odot}$ ). The effect,  $\Delta\tau_{p1}$ , on an interplanetary

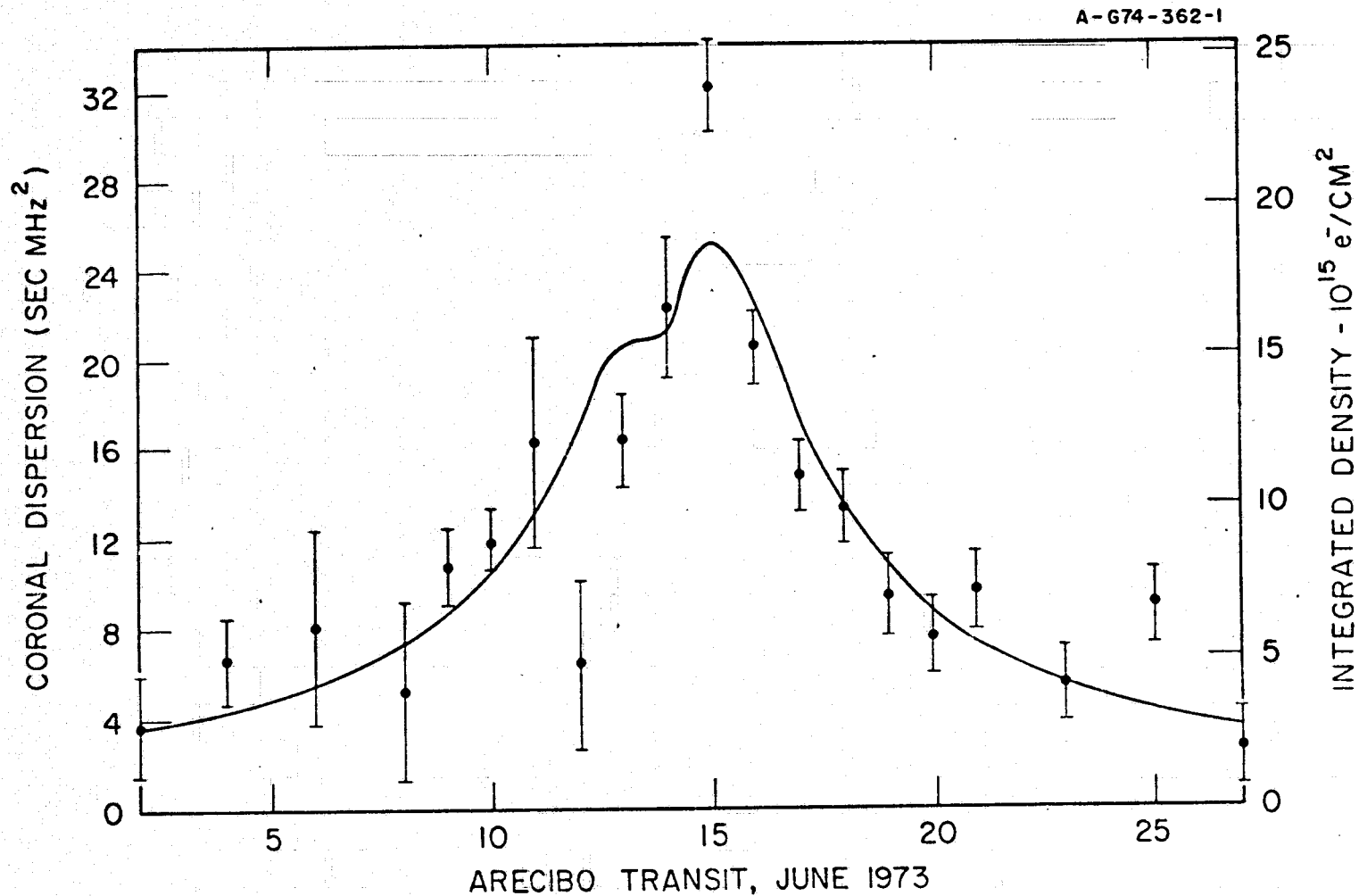


Figure 1. Integrated electron density through the solar corona as inferred from observations of the Crab pulsar surrounding its near occultation by the sun (5R = distance of closest approach) on June 15. The error bars represent one standard deviation and the solid curve corresponds to a theoretical model. (See Weisberg et al., 1975 for further details.)

time-delay measurement of such a plasma is given by (Shapiro, 1964):

$$\Delta\tau_{p1} \approx \frac{0.9 \times 10^{14}}{f^2} \left(\frac{R}{d}\right) \left[\tan^{-1}\left(\frac{x_e}{d}\right) + \tan^{-1}\left(\frac{x_p}{d}\right)\right] \text{ sec,} \quad (3.2)$$

where  $f$  is the radar frequency in Hertz,  $d$  is the distance of closest approach of the signal to the sun's center, and  $x_e$  and  $x_p$  are the distances to the earth and target planet, respectively, from the point on the signal path closest to the sun. [When the earth and target planet are both on the same side of the sun, for example, near inferior conjunction or opposition, Equation (3.2) must be modified to indicate that the absolute value of the difference of the two arctangents must be evaluated.] For  $x_e, x_p \gg d$ , we obtain near superior conjunction

$$\Delta\tau_{p1} \approx \frac{0.9 \times 10^{14}}{f^2} \left(\frac{R}{d}\right) \pi \text{ sec,} \quad (3.3)$$

showing that the plasma effect on time delay falls inversely with the impact parameter and with the square of the radar frequency. Since the predicted relativistic effect of solar gravity on signal delay,  $\Delta\tau_r$ , given in Equation (2.2), falls off logarithmically with  $d$  and is independent of frequency, the possibility for an accurate test clearly exists. For example, at the 7840 MHz frequency used

at Haystack,  $\Delta\tau_{pl} \approx 0.9 \mu\text{sec}$  for  $d = 5R_{\odot}$ , which is about 0.5% of the corresponding predicted general relativistic effect of about  $170 \mu\text{sec}$ . The signal-to-noise ratios achievable with the Haystack radar are, unfortunately, insufficient to take advantage of these favorable conditions. At S-band frequencies,  $\Delta\tau_{pl}$  doesn't even drop below 3% of  $\Delta\tau_r$  (with  $\gamma = 1$ ) until  $d \approx 20 R_{\odot}$  for which distance  $\Delta\tau_{pl} \approx 3 \mu\text{sec}$  and  $\Delta\tau_r \approx 115 \mu\text{sec}$ . This "cross-over" point is illustrated in Figure 2 for the S-band radar frequency of 2380 MHz to be used by the upgraded Arecibo facility and with Venus the target planet.

Because of the use of S-band at Arecibo, nowhere near the full advantage of the available signal-to-noise ratio can be taken in the performance of the time-delay, or signal-retardation, test of general relativity. For the other relativity tests which depend only on the orbital motion of the inner planets the situation is much ameliorated but the effects are still not negligible. For example, at the elongation of Mercury, Equation (3.2) shows that for  $f = 2380 \text{ MHz}$ ,  $\Delta\tau_{pl} \lesssim 0.3 \mu\text{sec}$ , whereas at inferior conjunction  $\Delta\tau_{pl} \lesssim 0.1 \mu\text{sec}$ . For Venus, the corresponding elongation and inferior conjunction numbers are slightly under  $0.15 \mu\text{sec}$  and  $0.04 \mu\text{sec}$ , respectively. For Mars at opposition, the most favorable case, we obtain  $\Delta\tau_{pl} \approx 0.03 \mu\text{sec}$ . The above results are summarized in Table 1.

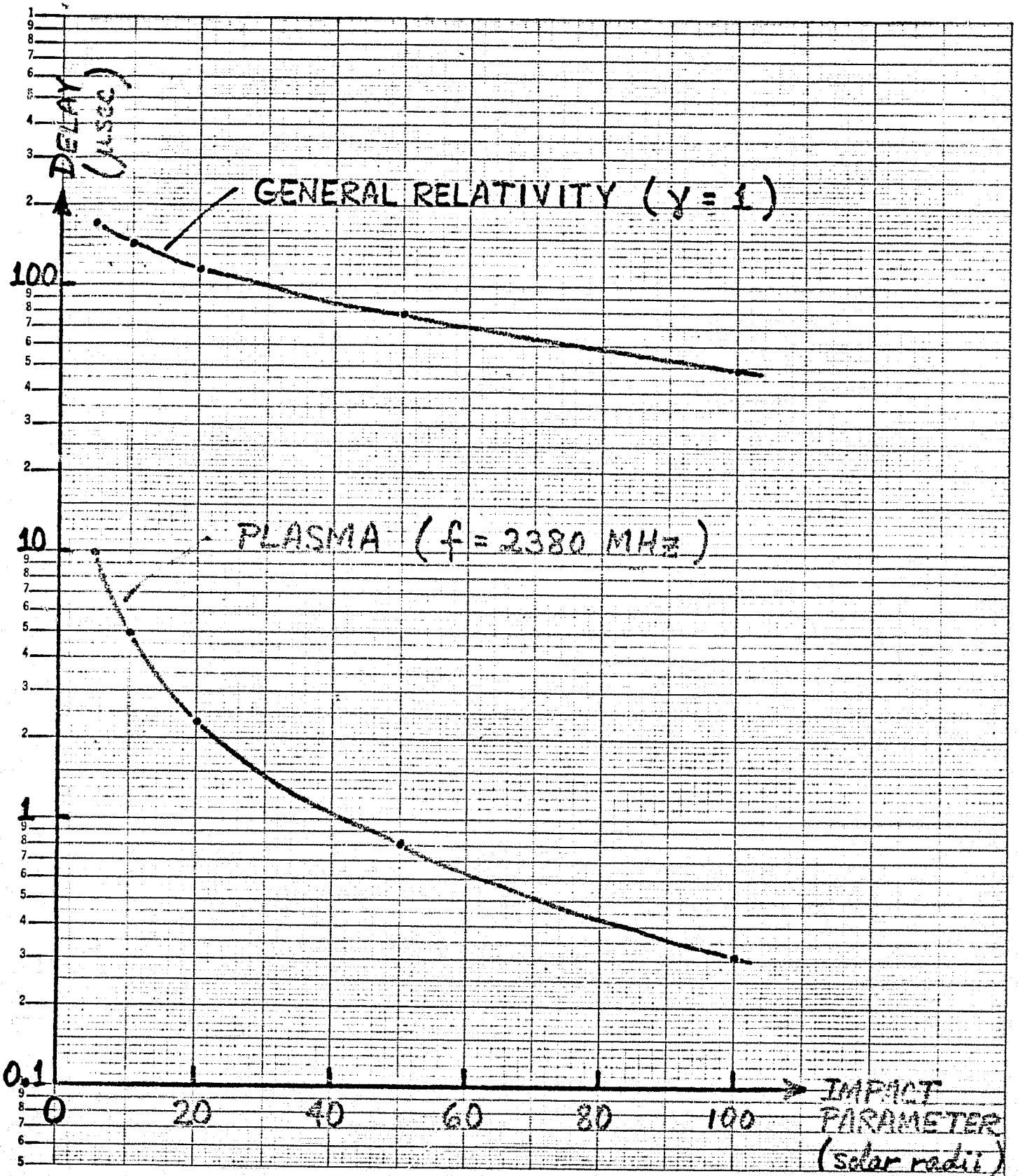


Figure 2. Time-delay effects for earth-based radar observations of Venus. The "plasma" curve represents the mean effect of the solar corona and the interplanetary medium.

SEMI-LOGARITHMIC 359-91G  
KEUFFEL & ESSER CO. MADE IN U.S.A.  
5 CYCLES X 70 DIVISIONS

Table 1. Average time delay, in  $\mu\text{sec}$ , expected from interplanetary plasma for 2380-MHz radar observations at different orbital configurations.

<u>Planet</u>	<u>Elongation</u>	<u>Inf. Conjunction</u>
Mercury	0.3	0.1
Venus	0.15	0.04
Mars	Opposition	
	0.03	



These estimates of the effects on delay of the interplanetary plasma between elongations and inferior conjunctions or oppositions are apt to be, on average, nearly a factor of two too large since Equation (3.1) yields a value for  $N$  of nearly  $11 \text{ el/cm}^3$  at 1 a.u., whereas the average value is perhaps only about 5 to  $7 \text{ el/cm}^3$ . Furthermore, using the plasma data obtained from the Pioneers and other relevant instruments, we should be able to model the plasma effects on delay with an uncertainty perhaps as low as 50%.

The above discussion demonstrates that the analysis and interpretation of radar data obtained in the past, with the exception of some Arecibo observations, have not been seriously compromised by the interplanetary plasma. Arecibo and, perhaps, Goldstone observations to be made in the future may be seriously affected. The most elegant way to virtually eliminate this corrupting effect is to make radar observations simultaneously, or nearly simultaneously, at two frequencies. At Goldstone there is now the capability to make observations at both S-band and at X-band. At the much more powerful Arecibo radar facility, only an S-band capability is currently planned. However, should the re-surfaced antenna at Arecibo be sufficiently well adjusted to be usable efficiently at X-band frequencies, an X-band radar system could be installed there too.

Delays measured simultaneously at two radar frequencies can be combined to yield a delay observable freed from plasma effects. The standard deviation,  $\sigma(\tau_f)$ , of this combined observable is related to the standard deviations  $\sigma(\tau_i)$ ,  $i = 1, 2$ , of the delays measured at the individual frequencies  $f_i$  by:

$$\sigma(\tau_f) \approx \left\{ \frac{f_2^4 \sigma^2(\tau_2)}{(f_2^2 - f_1^2)^2} + \frac{f_1^4 \sigma^2(\tau_1)}{(f_2^2 - f_1^2)^2} \right\}^{1/2}. \quad (3.4)$$

For  $f_1 \approx 2$  GHz and  $f_2 \approx 8$  GHz, Equation (3.4) yields

$$\sigma(\tau_f) \approx 1.07 \sigma(\tau_i), \quad (3.5)$$

for  $\sigma(\tau_1) \approx \sigma(\tau_2)$ . Thus the "penalty" paid in freeing the delay measurements from plasma effects is only about 7% for a dual, S- and X-band system.

For the purposes of the relativity tests, with X-band available, the S-band capability is not required except near superior conjunction where its effectiveness will cease only when the turbulence in the corona causes the delay measurement accuracy to decrease significantly. From elongation through inferior conjunction, even for Mercury, the maximum effect of the interplanetary plasma at X-band will be  $\Delta\tau_{pl} \approx 0.02$   $\mu\text{sec}$  which is nearly negligible.

#### 4. Gravitational Perturbations

The gravitational perturbations to the target planet and to the observing platform come from many sources: the galaxy, neighboring stars, the sun, the planets, asteroids, comets, and satellites. We treat each of these briefly in the order mentioned.

##### i. Galaxy

The galaxy introduces a gradient in the gravitational field so that the bodies in the solar system will thereby experience differential accelerations. For the purposes of an order-of-magnitude estimate we may consider the entire mass of the galaxy to be concentrated at its center. The magnitude of the differential acceleration,  $a_g$ , of a planet relative to the sun caused by the galactic mass will thus be given approximately by

$$a_g \approx 2 \frac{GM_g}{r_g^3} \Delta \quad (3.6)$$

where  $G$  is the constant of gravitation,  $M_g$  the mass of the galaxy,  $r_g$  the distance from the galactic center to the sun, and  $\Delta$  the distance between the planet and the sun.

Using the approximate values (see, for example, Allen, 1963)

$M_g \approx 10^{11} M_\odot \approx 2 \times 10^{44}$  gm and  $r_g \approx 9$  kpc  $\approx 3 \times 10^{22}$  cm, we obtain for Mars ( $\Delta \approx 2 \times 10^{13}$  cm), the outermost planet of interest, the value

$$a_g \approx 2 \times 10^{-17} \text{ cm/sec}^2 \quad (3.7)$$

since  $G \approx 6.7 \times 10^{-8}$  in cgs units. Since the most important, "in-plane" effect of this perturbing acceleration

will tend to average out over an orbital period, we can obtain a crude approximation to the magnitude of the effect by using the familiar formula  $s = (1/2)at^2$  with  $t$  being one-quarter ( $\approx 1.5 \times 10^7$  sec) of Mars' orbital period; we obtain

$$s_g \approx 2 \times 10^{-3} \text{ cm}, \quad (3.8)$$

which is utterly negligible. The gradient in the gravitational field due to neighboring galaxies is obviously far, far smaller.

#### ii. Neighboring Stars

Apart from the overall effect of the galaxy, one should, for completeness, estimate separately the influence of stars in the solar neighborhood. Using Equation (3.6) with  $M_g$  replaced by  $M_s$  and  $r_g$  by  $r_s$ , and with  $M_s \approx M_\odot$  and  $r_s \approx 1 \text{ pc} \approx 3 \times 10^{18} \text{ cm}$ , we obtain for Mars:

$$a_s \approx 2 \times 10^{-16} \text{ cm/sec}^2; \quad s_s \approx 2 \times 10^{-2} \text{ cm}, \quad (3.9)$$

again completely negligible. Thus, to this extraordinary degree, the solar system can be treated as a closed dynamical system.

#### iii. Sun

Here we are concerned with the gravitational effects of the sun on the motions of the planets, apart from the direct Newtonian and relativistic influences of an equivalent point mass. Three such effects are of potential significance: the mass distribution within

the sun, changes in the mass of the sun, and tidal bulges in the sun. We discuss each in turn.

iii. 1. Mass Distribution

The nonspherically symmetric part of the mass distribution of the sun has been the subject of considerable controversy over the past seven years.

Dicke and Goldenberg (1967) claim to have observed a visual oblateness of the sun and interpreted it, using Von Zeipel's theorem (see, for example, Clayton, 1968), to imply that the coefficient of the second harmonic of the sun's gravitational field had a value about two orders of magnitude larger than would be expected were the sun to be rotating uniformly with depth at the angular velocity observed at the surface. In particular, Dicke (1974) concludes that

$$J_{2\odot} \approx (2.4 \pm 0.3) \times 10^{-5} \quad (3.10)$$

where  $J_{2\odot}$  is the coefficient of the second-degree zonal harmonic in the usual spherical harmonic representation of the gravitational potential:

$$V(r, \theta, \phi) = - \frac{GM_{\odot}}{r} \left\{ 1 - J_{2\odot} \left( \frac{R_{\odot}}{r} \right)^2 P_2(\cos \theta) + \dots \right\}, \quad (3.11)$$

where  $R_{\odot}$  is the equatorial radius of the sun;  $r$ ,  $\theta$ , and  $\phi$  are the radius, colatitude, and longitude of the (external) field point; and  $P_2$  is the second-degree Legendre polynomial. [See, for example, Dwight (1949) for the normalization

used.] We have estimated the value for  $J_{2\odot}$  expected on the basis of uniform rotation and find

$$J_{2\odot} \approx 1 \times 10^{-7}, \quad (3.12)$$

with the uncertainty, even given uniform rotation, being perhaps as large as a factor of two.

Dicke's interpretation of the Princeton solar-oblateness measurements have been criticized by many. With the proper interpretation of the Princeton data in doubt, it is clear that other experiments are required. Older data, obtained with a heliometer over an 11-year period by Schur and Ambronn at the turn of the century, indicated the absence of any visual oblateness of the sun with an uncertainty several-fold below the magnitude of the effect reported by Dicke and Goldenberg. But Dicke has raised the possibility that systematic errors accompanying the use of the heliometers may have significantly affected this apparently null result. More recently, however, Hill et al.

(1974) using a technique very different from that employed at Princeton to define the solar limb, have also reported essentially a null result, supporting the earlier conclusions of Schur and Ambronn.

Regardless of the final outcome of the controversy surrounding the direct measurements of the visual oblateness of the sun, it is only the gravitational oblateness which is of concern for the radar tests of relativity. Since the gravitational oblateness characterized by  $J_{2\odot}$  can in any event only be inferred from the visual oblateness in a theory-dependent (and somewhat controversial) manner, we would like to be able to determine  $J_{2\odot}$  directly from its dynamical effects. The perturbations of the planetary motions due to  $J_{2\odot}$  are unfortunately smaller than those due to  $\gamma$  and  $\beta$  (see Section II). Even with  $J_{2\odot}$  as large as  $2.5 \times 10^{-5}$ , the perturbations of Mercury's orbit are only about 10% of those due to  $\gamma$  and  $\beta$ . With interplanetary time-delay measurements, the effects of  $J_{2\odot}$  can be separated from the relativistic ones due to the differences in

- (1) the dependence on orbital radius of the secular advance of the perihelion (the  $J_{2\odot}$  effect falls off faster by one power of the inverse radius);
- (2) the short-period perturbations of the orbits; and
- (3) the relations between or-

bital radius and period for a suite of planets. The relative efficacy of these differences in effecting a separation has never been studied with care. In particular, the relative importance for these differences of the "masking" effects of the orbital elements, which must be estimated simultaneously with  $J_{2\odot}$ ,  $\gamma$ , and  $\beta$ , has never been evaluated. But even after the relative efficacies have been determined, and a suitable strategy of observations adopted, and even if  $J_{2\odot}$  is of the order that one would predict from uniform rotation, the necessity for the precise determination of  $J_{2\odot}$  from its dynamical effects will likely remain the most important limitation so far mentioned on the accuracy achievable in the radar tests of relativity that involve planetary motions directly.

The third and higher-order harmonics of the sun's gravitational potential are obviously of no concern for the study of planetary motions. In addition to the overwhelming likelihood, based on theoretical considerations, that the coefficients will be much smaller than  $J_{2\odot}$ , their effects fall off with increasingly higher powers of the ratio of the sun's radius to the planet's orbital radius. Thus, even were  $J_{3\odot}$  of the same order as  $J_{2\odot}$ , the effect on Mercury's orbit would be almost two orders of magnitude smaller.

### iii. 2. Mass Changes

The second effect of the sun, mentioned at the start of this subsection, concerns its



change of mass. The main mechanisms for mass loss are electromagnetic radiation and the solar wind; the effects of neutrino radiation are negligible by comparison. Mass accretion takes place through direct impact of (perturbed) orbiting bodies and through the decay of the orbits of dust particles under the influence of the Poynting-Robertson effect (see, for example, Robertson, 1937). The losses can be evaluated more accurately than the gains. For electromagnetic radiation, we have

$$\begin{aligned} \left. \frac{dM_{\odot}}{dt} \right|_{\text{radiation}} &\approx -4\pi r_{\oplus}^2 \frac{I_{\odot}}{c} \approx -4 \times 10^{12} \text{ gm/sec} \\ &\approx -6 \times 10^{-14} M_{\odot}/\text{yr}, \end{aligned} \quad (3.13)$$

where  $r_{\oplus} \approx 1.5 \times 10^{13}$  cm is the radius of the earth's orbit;  $I_{\odot} \approx 2.0 \text{ cal/cm}^2\text{-min} \approx 1.4 \times 10^6 \text{ ergs/cm}^2\text{-sec}$  is the flux from the sun at 1 a.u.; and  $c \approx 3 \times 10^{10}$  cm/sec is the speed of light. We assume, of course, that the radiation is spherically symmetric. We make the same assumption, with substantially less reliability, for the particle flux in order to get a global estimate:

$$\begin{aligned} \left. \frac{dM_{\odot}}{dt} \right|_{\text{particles}} &\approx -4\pi r_{\oplus}^2 n m v \approx -2 \times 10^{12} \text{ gm/sec} \\ &\approx -3 \times 10^{-14} M_{\odot}/\text{yr}, \end{aligned} \quad (3.14)$$

where  $n \approx 10 \text{ cm}^{-3}$  is the (over) estimated average proton number density at 1 a.u.;  $m \approx 1.67 \times 10^{-24} \text{ gm}$  is the mass of a proton; and  $v \approx 400 \text{ km/sec}$  is the (over) estimated average velocity of the solar wind at 1 a.u. Particles other than protons make a much smaller contribution to the mass loss; their omission from  $dM_{\odot}/dt$  is far less serious than the uncertainty in the estimate of the proton mass loss.

The mass accretion is difficult to estimate reliably. Conceivably, but very unlikely, it might even exceed  $10^{-13} M_{\odot} \text{ yr}^{-1}$  and lead to a net mass gain for the sun. However current estimates (Marsden, 1974)

indicate a value for  $dM_{\odot}/dt|_{\text{influx}}$  of about  $10^{-15} M_{\odot} \text{ yr}^{-1}$  or smaller. For purposes of discussion let us assume that the change in mass of the sun, whatever its sign, doesn't exceed  $10^{-13} M_{\odot} \text{ yr}^{-1}$ . Such a bound implies that the uncertainty in the mass changes of the sun will not influence any of the radar tests of relativity for many years to come. The most pronounced effect of these mass changes will be a slow, outward spiralling of the planetary orbits which would affect most importantly the detection of any possible change in the gravitational constant. But even for radar time-delay measurements spanning two decades, the sun's mass changes, if within the limits specified, would introduce a maximum change in a delay measurement of under  $0.4 \text{ } \mu\text{sec}$ . For the near term, therefore, solar mass changes will not

limit the accuracy to which one can discern any possible change in the gravitational constant.

iii. 3. Tides

Tides are raised in the sun by the planets. Such tidal bulges affect the planetary orbits, in particular the semimajor axis, the eccentricity, and the inclination\*. However, the magnitude of these effects is negligible because of its dependence on both the square of the (small) planetary mass and the inverse sixth power of the ratio of the planet's distance to the sun's radius. This tidal effect on planetary orbits is also inversely proportional to the relevant "Q" of the sun. But even for  $Q \approx 10$ , likely a gross underestimate, and for Mercury, the most strongly affected planet, we find that the major effect, on Mercury's semimajor axis, is smaller than that due to the sun's mass loss and so may be neglected for the foreseeable future in regard to radar tests of relativity.

iv. Planets

The planets affect the radar time-delay measurements because of the perturbations they cause in the orbits of the earth and target planet. These effects, of course, depend on the masses and orbits of the perturbing planets. We discuss the orbits first. A third effect,

---

\* Because the planets are all beyond the radius of synchronous rotation with the sun, the orbits will tend to spiral out; they will also tend to circularize.

due to the spin-orbit coupling, will be discussed last.

iv. 1. Orbits

For the inner planets, where direct radar measurements exist for each, it is necessary to estimate simultaneously with the relevant parameters for the relativity tests the six orbital elements for each inner planet. These estimates must be based on the available radar and optical data concerning these bodies. It is desirable, but not mandatory, to include simultaneously in the analysis the optical data for the outer planets and the parameters describing their orbits (and masses). This expansion of the data and parameter sets in the solution is not now mandatory because the outer planets are of interest to the relativity tests under discussion only insofar as they perturb the orbits of the inner planets. But an error in an element of the orbit of an outer planet has only a second-order effect on the determination of the orbit of an inner planet. Nonetheless, the fractional uncertainties accompanying the radar time-delay observations of the inner planets are becoming so much smaller than those for the optical observations of the outer planets that, for example, the initial longitude of Jupiter in its orbit will soon be able to be estimated with higher accuracy from radar observations of Mars than from the existing optical observations of Jupiter. At this point the weak coupling between the inner

and outer planets will become sufficiently important to require a simultaneous solution in order to obtain an accuracy for the relativity tests commensurate with the inherent accuracy of the radar data.

Before this "crossover" point is reached, however, it may be possible, with the upgraded Arecibo radar facility to observe the Galilean satellites of Jupiter directly and possibly, also, Saturn's largest satellite, Titan. From the analysis of these direct radar measurements of the satellites of Jupiter and Saturn the orbits of the latter two will be determined far more precisely than would be possible from the inner-planet radar data. On the other hand, the inner-planet radar time-delay data, because of the much shorter distances involved and the inverse fourth power dependence of the echo strength on distance, will remain of far higher accuracy than the corresponding data from the outer solar system and so the latter data would add little to the determination of the orbit of the earth -- the common observing platform. This last statement also leads to the conclusion that, with no appreciable loss of accuracy, the inner-planet data can be analyzed separately from those of the outer planets for radar tests of relativity.

#### iv. 2. Masses

Several comments are required in regard to planetary masses. For the inner planets, radio-

tracking data from spacecraft near planetary encounters have yielded the masses for Venus, the earth, and Mars with uncertainties at the level of several parts per million (for a summary, see Ash, Shapiro, and Smith, 1971). Preliminary analysis of the Mariner 10 data (Howard et al., 1974) give an uncertainty for Mercury's mass of about 1 part in  $10^4$ . The radar time-delay data also contain information on these masses due to the perturbations induced by these planets in one another's orbits. Since these planets do not make close approaches, the spacecraft data are intrinsically more powerful for the estimation of planetary masses and all but eliminate the need to estimate them from the radar data. However, inclusion of the mass parameters in the analysis of the radar data for the relativity tests provides an important check on the existence of unsuspected systematic errors. Any disagreements between the "radar" and "spacecraft" values for the masses, large compared to the accompanying standard deviations, would imply the presence of such errors.

The outer planet masses are best determined from mutual perturbations among these planets, with two exceptions: Jupiter and Pluto. The mass of Jupiter (plus its satellites) is at present determined most accurately from analysis of asteroids whose mean motions are commensurable with Jupiter's.

The Pioneer 10 flyby of Jupiter provides the next most accurate value. For Pluto, despite some claims to the contrary (see, for example, Seidelmann et al., 1971), we have shown that its mass can not be determined reliably from its perturbations of the orbits of the other outer planets; Pluto's mass is simply too small and the optical observations of the outer planets are too crude to allow a determination (see Ash, Shapiro, and Smith, 1971). By the same token, Pluto is not massive enough to affect the radar tests of relativity.

As for the inner planets, however, the estimation of the masses of the outer planets from the inner-planet time-delay data provides a useful check. And, in fact, the formal accuracy achieved in such estimates of the masses of Jupiter and Saturn are only several-fold poorer than for the best now available.

#### iv. 3. Spin-Orbit Coupling

The spin-orbit resonance of Mercury (see, for example, Colombo and Shapiro, 1966; Goldreich and Peale, 1966; Counselman, 1968) is potentially of direct significance for radar tests of relativity. This resonance is responsible for a slight additional advance,  $\Delta\omega_{so}$ , of Mercury's perihelion given by

$$\Delta\omega_{so} \approx \frac{21\pi}{4e} \left(\frac{B-A}{C}\right) \left(\frac{R_g}{a}\right)^2 \cos 2\theta_0 \quad \text{rad/rev,} \quad (3.15)$$

where  $A < B < C$  are Mercury's principal moments of inertia;  $a$ ,  $e$ , and  $R_p$  are Mercury's orbital semi-major axis, eccentricity, and radius, respectively; and  $\theta_0$  is the angle between Mercury's axis of minimum moment of inertia and orbit major axis at perihelion. Since the value of  $(B-A)/C$  is unknown for Mercury, the precise magnitude of this effect can not be determined. However, based on analogy with the moon and on the likely extent to which Mercury could remain out of hydrostatic equilibrium over the relevant time interval, we conclude that  $(B-A)/C < 2 \times 10^{-4}$ . This bound on the fractional difference in the principal moments of inertia implies a perihelion advance of no greater than 0.003 per century. However, in order to improve the corresponding test of general relativity to the point where the uncertainty is a part in  $10^4$  or less, it will be important to have an independent estimate of  $(B-A)/C$  of uncertainty under  $2 \times 10^{-4}$ . Further analysis of the Mariner 10 radio tracking data obtained near Mercury encounters may yield a determination of sufficient accuracy; the corresponding data from an orbiter certainly will.

#### v. Asteroids

The asteroids, or minor planets, pose the same generic problems as the major planets. But because of their large number, their location in the solar system, and their small masses, the detailed problems posed



are quite distinct. A considerable effort has been expended under our direction (see Friedman, 1970, and Sherman, 1973) to develop the most feasible approach to include the asteroids in the data analysis. One cannot simply follow the "ideal" procedure and include all the asteroids in a grand and glorious N-body integration of the motion of the solar system bodies, with the associated orbital elements and masses added to the parameter set: N is just too large and, in fact, is not even known (except as a lower bound). As a reasonable compromise with practicality, we have chosen the apparently twelve most massive asteroids (see Allen, 1963, and also Matson, 1971, regarding the proper place of Bamberga), and we have taken their orbits as given by the separate reductions of the optical observations of these objects. Thus, in our integration of the planetary orbits, we include the effects of these asteroids on the planets, but ignore any possible corrections to the asteroid orbits that are implied by the (new) planetary orbits. This procedure is of more than sufficient accuracy for our purposes; the same arguments adduced for the major planets apply here, but a fortiori, since the proximity of the asteroids to the inner planets is, except possibly for a "pathological" case of near encounter, more than offset by the far smaller masses of the asteroids.

The masses of these dozen asteroids are set in accord with other determinations, based mostly on asteroid-asteroid perturbations, or estimates, based on measured diameters and an assumed density of  $3 \text{ gm/cm}^3$ . We also have the capability to add any subset of these masses to the list of parameters to be estimated in a given weighted-least-squares analysis of the data. The current limit of twelve could easily be raised to the order of thirty were such a change warranted.

What of the myriad of other asteroids? How can their effects be incorporated? We have chosen to replace the remainder of the asteroids by a circular mass ring whose radius, mass, inclination to the ecliptic, and longitude of the node can be either fixed or estimated as desired in any given analysis. The effects of the statistical fluctuations of the true asteroid distribution about this average ring must be evaluated in order to ascertain the usefulness of the ring model. (For a preliminary analysis, see Sherman, 1973.)

Finally, we comment on the magnitude of the asteroidal perturbations on the orbits of the inner planets. The largest asteroid, Ceres, has a mass of approximately  $6 \times 10^{-10} M_{\odot}$  (Schubart, 1974), which may represent about a third\* of the total mass of the asteroid belt. We can

---

\*This is the fraction inferred from Allen (1963), but it may be very unreliable.

make a crude estimate of the maximum effect its perturbations will have on inner-planet time-delay data, by evaluating the two-way light-time equivalent,  $\Delta\tau_{\text{Ceres}}$ , of the distance that Mars would be perturbed during a quarter of its orbital period if the acceleration due to Ceres acted in a constant direction with a magnitude corresponding to the distance of closest approach of the two objects (see Subsection III.4.i). We find:  $\Delta\tau_{\text{Ceres}} \leq 0.7 \mu\text{sec}$ . A more accurate, but still imprecise, bound obtained by comparison of two numerical integrations of Mars' orbit, one including and one omitting the effect of Ceres, yields a compatible bound.\* These numerical values indicate that the fractional error in the estimate of an asteroidal mass need be no less than about 0.1, except for the case of Ceres, in order to insure that, with the expected capability of the Arecibo radar system, no significant corruption of the radar tests of relativity will result. It is also clear that, for the same purposes, the gravitational effects of comets can be ignored. The corresponding effects of interplanetary "dust" have not been estimated explicitly but are presumably negligible.

#### vi. Satellites

The corrupting effects of satellites are most easily discussed by separating them into three classes: the moon, Phobos and Deimos, and the satellites of the outer planets.

---

\* This technique exaggerates the effect because of the drift in the planet's longitude due to the difference in total mass in the two calculations; this drift would largely disappear in an "operational" comparison.

vi. 1. The Moon

The moon affects interplanetary time-delay measurements primarily by causing the earth to revolve about the earth-moon barycenter. However, any inaccuracies in our knowledge of the geocentric orbit of the moon are reduced by a factor of 81 -- the earth-moon mass ratio -- in their effect on our calculation of the barycentric motion of the earth. Because of this nearly two order of magnitude reduction factor, only the lack of sufficient precision in knowledge of the earth-moon mass ratio and, to a lesser extent, in the moon's initial mean anomaly has been of any concern in the analysis of the interplanetary radar data. Thus these two parameters are included in the set to be estimated.

In the future, laser observations to the retroreflectors on the moon -- currently being made with errors of the order of only a few nanoseconds -- will yield an orbit that more than meets the accuracy requirements for the calculation of the earth's barycentric motion in the analysis of the radar data. The perturbations induced by the moon in the orbits of the other inner planets can, of course, be calculated with far higher accuracy than will be required by the interplanetary time-delay data.

vi. 2. Phobos and Deimos

Aside from our moon, Phobos and Deimos are the only known satellites of the inner planets.

These two satellites of Mars will, of course, cause Mars to rotate about the corresponding barycenter. The orbital radius of Phobos is only about 40% of that of Deimos, but the former's approximately five times larger volume (Duxbury, 1974) makes it, under the assumption of equal density, the greater contributor to the amplitude of Mars' barycentric motion. Assuming the density to be  $3 \text{ gm/cm}^3$ , we find that the amplitude of Mars' barycentric motion will be

$$\Delta\tau_b \approx \frac{2}{c} \frac{M_p}{M_M} a_p \approx 0.002 \text{ } \mu\text{sec} \tag{3.16}$$

where  $M_p \approx \frac{4}{3}\pi abc \rho \approx 1.8 \times 10^{19} \text{ gm}$  is Phobos' mass;

$M_M \approx \frac{2 \times 10^{33}}{3098700} \approx 6.5 \times 10^{26} \text{ gm}$  is Mars' mass;  $a_p \approx 9 \times 10^3 \text{ km}$

is the semimajor axis of Phobos orbit (Allen, 1963); and  $a \approx 13.5 \text{ km}$ ,  $b \approx 11.5 \text{ km}$ ,  $c \approx 9.5 \text{ km}$  are the principal axes of Phobos (Duxbury, 1974), with  $\rho$  its mean density.

Thus, for radar tests of relativity, Mars' barycentric motion is irrelevant.

We might also remark that any as yet undetected satellites of either Mercury or Venus would be too small to be relevant. For the likely limit on their size, such satellites could not be far enough from their parent planet to produce a noticeable effect, because orbits of that size would be unstable against solar perturbations.

vi. 3. Satellites of Outer Planets

The outer planets affect the presently contemplated radar tests of relativity only by their perturbations on the inner planets. To bound the corresponding effects of the satellites of the outer planets, we need only consider Callisto's effect on Mars' orbit. Because Callisto is in close orbit about Jupiter, the former's effect on Mars would be essentially quadrupolar. We can approximate the instantaneous acceleration exerted by Callisto on Mars by the simple, easily derived expression:

$$a_c \lesssim 3GM_c \frac{r_{J-G}^2}{r_{J-M}^4} \approx 10^{-13} \text{ cm/sec}^2, \quad (3.17)$$

where  $M_c \approx 10^{26}$  gm is Callisto's mass and  $r_{J-C} \approx 2 \times 10^{11}$  cm its mean distance from Jupiter (Allen, 1963), and where  $r_{J-M} \approx 3.7 \text{ a.u.} \approx 5.5 \times 10^{13}$  cm is the distance of closest approach of Jupiter and Mars. Considering Mars' orbital period, we find that the maximum effect on an earth-Mars time-delay measurement would be:

$$\tau_c \lesssim \frac{1}{c} a_c \left(\frac{P_M}{4}\right)^2 \approx 7 \times 10^{-4} \text{ } \mu\text{sec}, \quad (3.18)$$

where  $P_M$  denotes Mars' orbital period. Again we conclude that the problem caused by satellites is negligible. But in any event, we could calculate their effects to high accuracy so there is really no problem.

5. Non-Gravitational Perturbations

We consider now the direct effects of

nongravitational accelerations on the orbits of the inner planets. These come primarily from three sources: electromagnetic radiation, the solar wind, and particulate matter. The third category covers impacts on the planet of interplanetary dust, cometary material, and asteroids. We estimate the effects of each in this section.

i. Electromagnetic Radiation

The acceleration of a planet due to electromagnetic radiation (sunlight pressure) is proportional to the area-to-mass ratio of the planet and decreases inversely with the square of the distance to the sun. Of the planets of direct interest to us, Mercury is the most severely influenced by this perturbation and will be used to place an upper bound on it. We first consider the radial component of the pressure which produces an acceleration on Mercury equivalent to a slight decrease,  $\Delta M_{\odot}$ , in the mass of the sun.

We may bound this equivalent decrease by

$$\Delta M_{\odot} \lesssim 2G^{-1} \left(\frac{A}{M}\right)_{\oplus} \left(\frac{I_{\odot}}{c}\right) r_{\oplus}^2 \lesssim 1.8 \times 10^{20} \text{ gm}, \quad (3.19)$$

where  $(A/M)_{\oplus} \approx 5.6 \times 10^{-10} \text{ cm}^2/\text{gm}$  is the area-to-mass ratio for Mercury\*;  $(I_{\odot}/c) \approx 4.65 \times 10^{-5} \text{ dynes/cm}^2$  is the

---

\* By area, of course, we mean the projected area.

pressure of sunlight at 1 a.u., and  $r_{\oplus} \approx 1.5 \times 10^{13}$  cm is 1 a.u., the semimajor axis of the earth's orbit. The factor of two on the right side of Equation (3.19) reflects the overestimate (upper bound) based on conditions of "flat-plate" reflection. The magnitude of the effect on time-delay measurements from earth to Mercury of this effective decrease in the solar mass, a radial acceleration, can be bounded by

$$\Delta\tau_{sr} \lesssim \frac{2\pi}{c} r_{\oplus} \left(\frac{\Delta M}{M}\right)_{\oplus} \frac{t}{P_{\oplus}} \approx 5 \times 10^{-4} t \mu\text{sec}, \quad (3.20)$$

where  $r_{\oplus} \approx 0.6 \times 10^{13}$  cm is the semimajor axis of Mercury's orbit;  $P_{\oplus} \approx 0.24$  years is Mercury's orbital period; and  $t$  is expressed in years. (Note that the factor of two introduced by round-trip delay is cancelled by a factor of one half introduced by the relation between the sensitivity of the rate of change of longitude displacement to the effective change in solar mass.) For radar observations spanning several decades, this sunlight-pressure perturbation can be ignored.

There is the possibility that the reflection properties of Mercury, for example, could be sufficiently "skewed" for the reflected radiation to cause the average acceleration vector to have a substantial fractional component in the tangential direction that is parallel to Mercury's direction of motion. (All surface longitudes on Mercury do not receive equal amounts of solar illumination, either in magnitude or direction, because of the spin-orbit resonance and the orbital eccentricity. Thus, even if the surface reflected isotropically, longitude variations of albedo could result in a nonzero-average tangential radiation.)



Displacements due to such accelerations grow, of course, quadratically with time. Thus a bound similar to that given by Equation (3.20) can easily be derived for the tangential acceleration:

$$\Delta\tau_{st} \lesssim \frac{G}{c} \Delta M_{\odot} \frac{F}{r_{\odot}^2} t^2 \approx 1.1 \times 10^{-2} F t^2 \mu\text{sec}, \quad (3.21)$$

where  $F$  is the fraction representing the ratio of the magnitude of the tangential acceleration due to sunlight pressure to that of the total due to sunlight pressure. The time,  $t$ , is again given in years. For  $F$  of the order of 0.01, which is much higher than crude estimates would indicate, a set of radar observations spanning more than a decade might begin to be noticeably affected by such a tangential acceleration.

A related source of a tangential acceleration is the infrared radiation from a planet with a temperature distribution asymmetric with respect to the sun-planet line. We can place a crude upper bound on this acceleration with the following easily-derived formula:

$$a_{ir} \lesssim \frac{3\sigma T^3 \Delta T}{c} \left(\frac{A}{M}\right)_{\dagger} \approx 3.4 \times 10^{-14} \text{ cm/sec}^2, \quad (3.22)$$

where  $\sigma \approx 5.67 \times 10^{-5} \text{ ergs/cm}^2\text{-deg K}^4\text{-sec}$  is the Stefan-Boltzmann constant,  $T \approx 600^\circ\text{K}$  is an upper limit on the average surface temperature on Mercury,  $\Delta T \approx 50^\circ\text{K}$  is an

upper limit on the average difference in temperature between the "leading" and "trailing" hemispheres of Mercury; and, as stated above,  $(A/M)_{\oplus} \approx 5.6 \times 10^{-10} \text{ cm}^2/\text{gm}$  is the area-to-mass ratio for Mercury. In this approximation, Mercury is being treated somewhat like two flat plates whose normals are in the direction of orbital motion and whose areas are equal to the projected area of Mercury.

The maximum effect on the earth-Mercury time-delays of this "infrared" acceleration is given by:

$$\Delta\tau_{\text{ir}} \lesssim \frac{1}{c} a_{\text{ir}} t^2 \approx 0.001 t^2 \text{ } \mu\text{sec} , \quad (3.23)$$

where  $t$  is measured in years. If this upper bound actually represented the effect, we can see that the interpretation of a span of data more than a decade in extent would begin to be seriously affected by this infrared radiation. Thus, a more careful bound on this effect should be developed before too long a span of data is analyzed.

Finally, we note that the Poynting-Robertson effect (Robertson, 1937), mentioned earlier, also introduces a tangential acceleration but smaller in magnitude by a factor of about  $v/c$  relative to the radial acceleration due to sunlight pressure. Thus,

$$a_{\text{pre}} \lesssim 2 \left( \frac{v_{\oplus}}{c} \right) \left( \frac{A}{M} \right)_{\oplus} \left( \frac{I_{\odot}}{c} \right) \left( \frac{r_{\oplus}}{r_{\oplus}} \right)^2 \approx 5 \times 10^{-17} \text{ cm/sec}^2 \quad (3.24)$$

where  $v_{\oplus}$  is the orbital velocity of Mercury and  $(r_{\oplus}/r_{\oplus})$  is

the ratio of the earth's orbital semi-major axis to Mercury's. This acceleration is clearly negligible compared to the upper bound calculated above for the infrared radiation. The orbital effects of the cosmic background black-body radiation are also negligible.

### ii. Solar Wind

To obtain approximate values for the effects of the solar wind on planetary orbits, we follow the same procedures as used in Subsection 4. iii.2. If we assume that the solar wind impinging on a planet's surface is completely absorbed (we can ignore the effects of the resultant increase in mass of the planet), then we can approximate the radial acceleration due to the wind by

$$a_{wr} \approx \left(\frac{A}{M}\right)_{\oplus} (nmv^2)_{\oplus} \approx 6 \times 10^{-17} \text{ cm/sec}^2, \quad (3.25)$$

where  $(nmv^2)_{\oplus}$  represents the radial momentum transfer to the planet per unit area per unit time; and where, individually,  $n \approx 70$  particles/cm<sup>3</sup> is the density of protons in, and  $v \approx 300$  km/sec the speed of, the solar wind at Mercury's orbit with  $m \approx 1.67 \times 10^{-24}$  gm being the mass of a proton. To the extent that  $(nmv^2)$  might be constant over Mercury's orbit, the effect of  $a_{wr}$  on the orbit would be of short period only. In this case, we can place an upper bound on the consequent effect on time delays by using the "s =  $\frac{1}{2}$  at<sup>2</sup>" method with  $t$  one quarter of Mercury's orbital period. We find  $\Delta\tau < 10^{-8}$   $\mu$ sec, which is completely negligible. To the extent that  $nmv^2$  varies inversely with the

square of Mercury's distance from the sun we have a bound similar to that given by Equation (5.2), except that the wind's effect is smaller by a factor

$$\frac{a_{wr}}{a_{sr}} = \frac{(nmv^2)_{\oplus}}{2 \left(\frac{I_{\odot}}{c}\right) \left(\frac{r_{\oplus}}{r_{\odot}}\right)^2} \lesssim 2 \times 10^{-4}, \quad (3.26)$$

where values for the various quantities were given above.

For completeness we also point out that, due to aberration, the solar wind causes a tangential acceleration as well, given approximately by:

$$a_{wt} \approx \frac{v_{\oplus}}{v_w} a_{wr} \approx 1.5 \times 10^{-17} \text{ cm/sec}^2, \quad (3.27)$$

where  $v_{\oplus} \approx 50$  km/sec is Mercury's orbital velocity and  $v_w \approx 300$  km/sec is the velocity of the solar wind at Mercury's orbit. Comparison with Equation (3.24) shows that  $a_{wt}$  is about a factor of three smaller than the corresponding acceleration due to the (negligible) Poynting-Robertson effect.

Although no explicit bounds have been calculated, it is probably quite safe to conclude that the effects of the magnetic field and of the particles in the solar wind on the planetary magnetospheres (where they exist) introduce no discernible effects on the orbits of any of the inner planets. Similarly, we conclude that the effects of cosmic rays are negligible.

### iii. Particulate Matter

It is difficult to estimate reliably the momentum transfer and mass changes that accrue from collisions between planets and interplanetary dust,

comets, and asteroids. According to Marsden (1974), the influx of such material on the earth at present probably averages no more than about  $5 \times 10^{12}$  gm/yr. The consequent fractional mass change in the earth of  $10^{-15}$  yr<sup>-1</sup> will have negligible import for tests of relativity as can be seen from analogy with the discussion in Subsection 4.iii.2. momentum transfer to the earth is undoubtedly a minuscule fraction of the total of the magnitudes of the momenta of the individual particles. However, even if the net transfer were equal to this total, the effect on the earth's orbit would be small. Taking 20 km/sec as the maximum relative velocity,  $v_r$ , and assuming all these velocities to be parallel to the earth's orbital velocity, we obtain a gross upper bound on the tangential acceleration due to particulate matter of

$$a_{pt} < \frac{v_r \dot{M}_{\oplus}}{M_{\oplus}} \approx 5 \times 10^{-17} \text{ cm/sec}^2, \quad (3.28)$$

where  $\dot{M}_{\oplus} \approx 1.7 \times 10^5$  gm/sec is an upper bound on the rate of mass gain by the earth as estimated above. Comparison with the previous subsection shows that even if this upper bound were the actual tangential acceleration, the latter would have negligible effects on the relativity tests. We may also reasonably conclude that the influx of particulate matter on the other inner planets can also be neglected. Only Mars is likely to have a substantially higher influx than the earth, but not by a factor large enough to render invalid the above conclusion.

Any, perforce infrequent, collisions between inner planets and large objects ( $\geq 10$  km in diameter and  $1.5 \times 10^{18}$  g in mass) could be modelled as impulses in the analysis.

## 6. Planetary Topography

Perhaps the most vexatious problem hindering the maximum utilization of radar data for testing general relativity is that caused by the large topographic variations over the surfaces of the target planets. Mars, the worst offender, introduces variations in the time delays of up to about  $\pm 50 \mu\text{sec}$ . Fortunately, these topographic variations over the surface are constant in time, at least on scales of current interest for radar tests of relativity. Still, we can not simply conclude that, once determined, topography is of no further concern as a corrupting effect. The effective time delay measured by a radar system is not only influenced by the coding of the waveform (see, for example, Pettengill, 1971), but also by the radar scattering law obeyed by the surface. This scattering law, in general, depends on the frequency of the impinging radio waves, on their polarization, and on the angle of incidence. A generalized mapping of the relevant part of the surface of each target planet to the resolution possible with the signal-to-noise ratio available is an enormous, but by no means impossible, task.

In the remainder of this subsection, we shall discuss the various radar methods of measurement which can yield information on the topography as well as the methods so far developed for analyzing these data to separate the (unwanted) planetary topographic information from the (wanted) planetary orbital information.

### i. Methods of Measurement

There are a number of different methods that have been utilized to glean topographic information

from radar echoes. We will summarize very briefly three that relate, respectively, to topography at the subradar point, along the so-called Doppler equator, and over the visible hemisphere. The first two are being used routinely in planetary observations. The third has so far only been applied successfully to the moon since the signal-to-noise ratio requirements have been heretofore too severe for planetary application.\*

i. 1. Topography at the Subradar Point

Consider a radar that transmits a sequence of short pulses of radio energy, or a phase-coded continuous-wave signal (see, for example, Evans and Hagfors, 1968), towards a planet. To determine the time delay of the reflection from the subradar point of these signals, a number of different techniques have been employed. We shall describe only one: The (decoded) echo power, as a two-dimensional function of time delay and Doppler shift, is cross-correlated with a parameterized model of the expected function. As presently implemented, for example at the Haystack Observatory, the parameter set includes one each for the time delay and Doppler shift corresponding to reflections from the subradar point, and others to describe the average, and assumed uniform, scattering law of the surface at the subradar point and in the surrounding regions that contribute appreciably to the echo. The values

---

\*A variant of this method has recently been applied with success in a radar experiment with Venus the target (R.M. Goldstein, 1975). Two antennas of the Goldstone Tracking Station were used to form the needed interferometer (see Subsection 6.i.3).

of the parameters which maximize the cross-correlation function are good approximations to the maximum likelihood estimates. The estimate for the time delay to the sub-radar point, of course, contains, additively, the effects of the topography there. Each observation, however, gives a delay averaged relative to that portion of the surface that passed through the subradar point during the observation. Thus, the "footprint" on the target planet's surface for a delay observation depends on the duration of the observation as well as on the effective pulse length and frequency resolution of the radar system. The minimum useful duration of the observation is limited primarily by signal-to-noise considerations; usually sufficient integration time is employed to insure that the interpretation, or analysis, of the measurement will not be limited by such a consideration. For Mars, the integration time employed is usually far less than for Mercury and Venus because the rotation rate of Mars is so much more rapid\*. To develop this comparison quantitatively, consider the approximate resolution on the surface afforded by a pulse length (or code-element length for continuous-wave signals) of  $\Delta\tau$  and a frequency resolution of  $\Delta f$  for a radar system operating at a radio frequency  $f$ . Simple

---

\*Of course, if sufficiently accurate knowledge of relative topography were available in a region, the integration could be extended over a longer period of time with no consequent sacrifice in the interpretation.



geometrical arguments show that

$$\Delta S = 2(2cR_p \Delta\tau)^{1/2} \quad (3.29)$$

and

$$\Delta L = \frac{c\Delta f}{2\omega_p f} \quad (3.30)$$

where  $\Delta S$  represents the diameter of the spot, centered at the subradar point, that is "illuminated" simultaneously, or "encompassed", by the pulse of length  $\Delta\tau$ ; and  $\Delta L$  represents the length, measured along the Doppler equator\*, of the arc whose points impart a Doppler shift to the echo that lies between  $\pm\Delta f/2$  of the Doppler shift for the subradar point.

---

\*The Doppler equator passes through the planet's center of mass and is normal to the axis that results from the projection of the "apparent" angular velocity vector onto the plane normal to the earth-planet line. The "apparent" angular velocity vector is the angular velocity vector of the planet as viewed from the radar site and contains contributions from the relative orbital motions of the planet and site as well as from the planet's sidereal rotation.

The quantities  $R_p$  and  $\omega_p$  represent, respectively, the radius of the planet and the magnitude of the projection of the apparent angular velocity vector along the Doppler axis. From the relation

$$\Delta L \approx \omega_p R_p t \quad (3.31)$$

we can estimate the limit on integration time,  $t$ , necessary to prevent the surface resolution inherent in the values of  $\Delta\tau$  and  $\Delta f$  from being "smeared".

Thus, for  $\Delta\tau \approx 1 \mu\text{sec}$ ,  $f \approx 2380 \text{ MHz}$ , and  $\Delta f \geq 0.1 \text{ Hz}$ , which would be available initially for the upgraded Arecibo facility, we obtain the surface resolutions and integration-time limitations shown in Table 2 for each of the inner planets. Scaling to other values for the radar resolutions follows from Equations (3.29) and (3.30). Aside from the consideration of integration time, the equations show that the better the time resolution the smaller the area of the surface whose average topography affects the delay measurement. The "vicious cycle" nature of this fact will be explored in Subsection 6. ii.

i. 2. Topography Along the Doppler Equator

Through use of a procedure for data analysis different from the one described above, information on the relative topography along the Doppler

Table 2

Surface Resolution and Integration-  
Time Limitations for Future Arecibo  
Radar Observations of the Inner Planets\*

<u>Planet</u>	<u>Surface Resolution</u> (km)	<u>Integration Time Limit</u> <u>to Avoid "Smearing"</u> (hours)
Mercury	77	7.1
Venus	120	16.3
Mars	90	0.1

---

\* Calculation based on an effective pulse length,  $\Delta\tau$ , of 1  $\mu\text{sec}$  and a frequency resolution,  $\Delta f$ , which matches the "Doppler" surface resolution,  $\Delta L$ , to the "delay" surface resolution  $\Delta S$  [see text, Equations (3.29) and (3.30)].

equator can be obtained from the radar signals reflected from the planet. The basic idea can be outlined as follows: The echoes, after suitable coherent integration, are segregated by frequency, or Doppler shift. Echoes with a given Doppler shift can easily be shown (see, for example, Evans and Hagfors, 1968) to have been reflected from a "strip" along the planet's surface that lies in a plane parallel to the one containing both the vector from the radar site to the planet's center and the planet's apparent angular velocity vector. The distance of the strip from the Doppler axis (which, in projection, contains the sub-radar point) is proportional to the relative Doppler shift of the strip and the subradar point. Having isolated the power by frequency, we may then examine it as a function of delay. The consequent curve will exhibit a steep rise from the noise level at the delay corresponding to the region near the Doppler equator, followed by a moderately slow decline in echo power for greater delays. In the idealization of a noise-free spherical-target situation, the first echo received at a given Doppler shift will be from the point on the Doppler equator that imparts this particular Doppler shift. Reflections from other points on the Doppler strip will arrive later since they lie at greater distances from the radar site. If the point under discussion on the actual

Doppler equator lies above or below the model spherical surface the echo will begin to arrive earlier or later. (A more accurate estimate of this time can in general be obtained by cross correlation of the echo for the Doppler strip with a suitably parameterized model profile based on the average scattering law for the planet.) By a comparison, then, of the time of arrival of the first echo from a particular Doppler strip with the corresponding time of arrival of the first echo from the Doppler shift corresponding to the subradar point, we can deduce the relative topography of the two points, after correction for the spherical effect. In this manner, from a single observation, we can deduce the relative topography along an arc of the Doppler equator. The useful length of the arc, in general symmetrically placed with respect to the subradar point, will depend on the available signal-to-noise ratio. The scattering laws for the inner planets show, for example, that the echo power from the limb of each planet is lower than that from the subradar point by from 30 to 40 db\*. Current observations have typically yielded useful topography for arcs of up to  $\pm 10^\circ$ .

---

\* We exclude here observations of Venus at X-band for which the decline of echo power is more precipitous due to the added effects of the atmospheric absorption.

The results obtained with this approach are subject to distortion from several different sources: (1) An error in the assumed Doppler shift to the subradar point will cause a misidentification of the relation between Doppler shift and surface points along the Doppler equator with the consequence that the profile of topography will have an overall slope relative to the profile that should have been obtained; (2) The presence of anomalously high topography near, but not on, the Doppler equator or, conversely, the presence of an anomalously deep depression on the Doppler equator will cause the first echo for that Doppler shift to be associated with a point off the Doppler equator rather than on it as assumed in the interpretation; (3) The presence near or on the Doppler equator of a surface region with unusual back-scattering properties could lead to false identifications of the first echo as described above; and (4) Depending on the radar parameters, "aliasing" in delay and frequency can be present and may cause echoes from different regions of the planet to be "lumped in" with the echoes from the strip under consideration. This fourth difficulty can be surmounted to a great extent by proper choice of radar parameters, although the size and rotation rate of the planet may impose certain limitations (see, for example, Shapiro et al., 1972 a, and Evans and Hagfors, 1968).

The other potentially distortive effects can be guarded against by careful comparison of the results from a number of observations carried out with slightly different orientations of the Doppler equator relative to the planet's surface and with different positions of the subradar point. Comparison between observations at neighboring subradar points can be done for Mars on the same day, because of its rapid rotation, as well as on different days. But for Mercury and Venus whose rotation periods are comparable to the orbital periods, one relies on observations on adjacent or nearly adjacent days. Because, at a given site, observations can extend over only a relatively small fraction of the day some surface regions on these two planets will pass through the respective subradar points when observations are impossible. Therefore "overlap" will be incomplete; nevertheless sufficient overlap exists, even in the worst case, to insure reliability. With the upgraded Arecibo facility, the useful arclengths along the Doppler equator will be severalfold greater and will yield more overlap. The comparison of the results for topography for points along the Doppler equator, determined from one observation, with the results for the same points, obtained as they passed through the subradar point, provides an important check since many of the sources of systematic errors are different for the two methods. (Of course, these checks are limited to those sets of surface points that, at different times, lie both at the subradar point and at other

positions along a Doppler equator.)

i. 3. Topography Over the Visible Hemisphere

Finally, we present a brief description of a third technique to determine topography from radar observations. It is more sophisticated than either of the two described above, but has so far been applied usefully only to observations of the moon (Shapiro et al., 1972a; Zisk, 1972). Called delay-Doppler interferometry, this method, at least in principle, allows the topography over a large area of the visible hemisphere to be determined in one observation, and the topography over the whole sphere to be determined in a series of observations. The method is based on the simultaneous determination of each of three coordinates of a reflecting region on the surface. One coordinate is provided by the echo delay and a second by the Doppler shift. These two coordinates combine to localize the echo to a "stick" which represents the intersection of the delay contour, which is a plane normal to the radar site-planet vector, and the Doppler-shift contour, which is a plane parallel to that formed by the radar site-planet vector and the planet's apparent angular velocity vector. The third coordinate is provided by interferometry. With a second antenna connected interferometrically to the first, and receiving the same echo as the first antenna, one can determine the fringe phase for



the reflecting region isolated by the delay-Doppler coordinates. If the baseline between the two antennas, when projected onto the plane normal to the radar site - planet vector, is parallel to the delay-Doppler stick then maximum resolution is obtained along the stick. Quantitatively, this resolution is:

$$\Delta H \approx \frac{R\lambda\Delta\phi}{2\pi B_p}, \quad (3.32)$$

where  $R$  is the earth-planet distance,  $\lambda$  is the wavelength of the radio signals,  $B_p$  is the projection of the baseline along the delay-Doppler stick, and  $\Delta\phi$  is the uncertainty in the estimate of the fringe phase. For observations of Venus near inferior conjunction with the upgraded Arecibo radar facility and its planned outrigger antenna, we would have as typical values:  $R \approx 0.3 \text{ a.u.} \approx 5 \times 10^{12} \text{ cm}$ ;  $\lambda \approx 15 \text{ cm}$ ;  $B_p \approx 20 \text{ km} = 2 \times 10^6 \text{ cm}$ ; and, perhaps,  $\Delta\phi \approx 0.005 \text{ radian}$ .\* Thus,  $\Delta H \approx 300 \text{ m}$  which is too crude to be very useful for the high accuracy required in the radar tests of relativity.

---

\* Note that the usual  $2n\pi$  fringe phase ambiguity, where  $n$  is an unknown integer, is not a factor in these monochromatic observations because the a priori uncertainty in the topography is considerably smaller than the corresponding interval between ambiguities.

If, however, the Arecibo and Haystack radars were used to form the interferometer and if, further, the Arecibo radar were instrumented to transmit and receive at an X-band frequency ( $\lambda \approx 3$  cm), then the resolution along the Doppler stick afforded by the fringe-phase measurement might be reducible from about 300 m to the order of 10 m which would be useful for the relativity tests. Of course, with this much higher resolution the ambiguity problem\* is no longer completely ignorable, although it is still not serious.

The effect of fluctuations in Venus' atmosphere on the phase of the interferometric signals should not be serious (Shapiro et al., 1972a) because the paths from any resolution cell on the surface to the two radar receivers on earth could never be separated by more than about  $10^{-4}$  radians and probably by one or so orders of magnitude less. Because of the near coincidence of these paths in the atmosphere of Venus, its influence on the phase delays to the two receivers should cancel almost completely when the signals are cross correlated to obtain the fringe-phase observable.

---

\* See footnote on p. 80.

The effects of the earth's atmosphere could be more serious; however, near cancellation can be achieved by use of specially chosen surface resolution cells as phase calibration points (Counselman et al., 1972; Shapiro et al., 1972a).

Before concluding this discussion of the delay-Doppler-interferometry method of topography determination, we comment briefly on the interpretation of the three coordinates measurable by radar: The delay coordinate can be interpreted directly in terms of a spatial coordinate; it is essentially the distance to the reflection point (for a more precise description, see Shapiro et al., 1972a). The interpretation of the Doppler coordinate in terms of a spatial one depends not only on the frequencies of the transmitted and received signals, but also on the (precalculated) radar site-planet vector and apparent angular velocity vector. The interpretation of the fringe-phase coordinate, as described above, in terms of a spatial coordinate will depend not only on the interpretations of the delay and Doppler coordinates but as well on the baseline vector that connects the interferometer elements and, to a lesser extent, on the (geocentric) angular velocity of the baseline vector. Thus only for the delay measurement is the interpretation in terms of a spatial coordinate reasonably direct and free from the need for knowledge of other quantities.

#### ii. Methods of Analysis

We shall now discuss the various approaches that have been either used or proposed

to try to eliminate or at least to reduce the effects of topography on the results of the radar tests of relativity. We base the discussion on only the two types of delay data discussed above: time-delay measurements to the subradar point and time-delay measurements corresponding to a particular Doppler shift different from that of the subradar point\*. The appropriate generalization of method to include data of

---

\* Note that this second type was considered in the earlier discussion only insofar as it yielded topographic information relative to that from the subradar point. However, the second type of delay, like the first type, can also be considered as an "absolute" observable and we adopt this viewpoint here. There remains an important difference between the two types: Data of the first type can, in effect, stand alone with the exception noted below; data of the second type require the auxiliary Doppler information so that the coordinates on the surface to which the measurement refers can be determined. Aside from the consequences, discussed previously, of a misidentified Doppler shift, which affects only the second type of delay data, both types are affected by errors in the knowledge of the planet's rotation vector. At present this uncertainty is no problem; with improved accuracy in the surface resolution of the delay data, it could conceivably become a problem for Venus. In this eventuality the Venus radar data themselves could be used to improve the estimate of the rotation vector.

the third type, not yet available from planetary observations, should be obvious from context.

The simplest approach is to ignore topography and to analyze all of the delay data based on the model of spherical planets, the assumption being that the topographic effects will tend to average out and will not seriously affect the relativity test results. In earlier times, when the uncertainty in individual measurements of delay was comparable to the variation in delay imparted by topography, this approach was adequate. Computer experiments have shown that with the more accurate data already available, the correlations of the topography with the parameters that characterize the relativity tests are high enough to have a large degrading influence on these tests.

The second approach involves the use of a parameterized model of the topography. One can, for example, use a spherical harmonic expansion over the whole sphere or use a two-dimensional Fourier series representation confined to the equatorial belt on the planet that contains all possible subradar points. We have tried both of these parameterizations and have found the latter, augmented by "flattening" parameters, to be the more useful because of the restricted coverage of the surface afforded by the subradar points. Nonetheless, such models have a serious practical defect: only the relatively low frequency com-

ponents of the global topography can be modelled in this manner because of the rapid increase in the number of parameters with increased resolution. Thus, to achieve a  $10^\circ \times 10^\circ$  resolution on the surface with the model we need, in our Fourier series approach, about 120 parameters. Of course, for all three target planets combined, the number of topography parameters will be about 360. (This number can be comfortably handled in our present analysis program; the matrix inversion for the weighted-least-squares analysis for the total of over 400 parameters needed for the description of the orbits, etc., as well as of the topography, requires only a few minutes of computer time.) Such a low resolution, however, can not possibly account, for example, for the myriad small craters which are very noticeable even with delays measured at presently achievable accuracies. To compensate for this deficiency in the parameterization, the errors associated with the delays in the analysis can be raised to a level comparable to the magnitude of the unmodelled topographic variations. Full advantage will then not be taken of the inherent measurement accuracy. It appears that the radar tests of relativity are therefore limited by these unmodelled "high-frequency" terms in the topographic variations and so other techniques to compensate for this defect are now being applied. We shall describe two such techniques below.

Consider first two delay measurements to a given planet made at widely separated times but with the same radar parameters and with respect to the same subradar point. From these two observables, two different observables can be formed: the difference observable and the sum observable. The former, of course, is simply the difference between the original two observables with the latter having a corresponding interpretation. The point of this transformation is that the difference observable is independent of topographical effects since they enter precisely the same way in each of the two original observables. The difference observable could be used in the analysis with its full weight, considering only the measurement error contributions to its uncertainty. No allowance in the weighting need be made for the high-frequency components of topography being unmodelled.

If every delay measurement had a "mate" in the sense just described, the topography problem would be solved in a satisfactory manner. The difficulty is that no delay measurement has a precise mate and only relatively few have near mates. In this situation, several types of options are open:

- (1) Ignore all observations that do not have a mate, where "mate" is now less precisely construed to mean an observation made with respect to a subradar point that falls within a certain specified angular separation of the subradar point of the companion observation. For these "mated" observations,

or "closure" points, analyze only the difference observables and ignore any topographical variations that may exist between the two subradar points associated with the original observations that were used to form the difference observable; (2) Introduce the concept of a (possibly variable) correlation length for topography on each planet. In particular, one can continue to use a parameterized model for the topography, but consider all delay measurements to a given target planet to be correlated. The correlation coefficient for each such pair of delay measurements can be related to the angular separation of the corresponding subradar points and to either a fixed or variable correlation length.

Both of the options described above are being investigated. The main difficulty is the lack of a sufficiently large number of near mates or closure points. The basic geometry of radar site and planet, to say nothing of the difficulties in scheduling observations, severely limits the possibilities. For Mars the geometric cause is the drift in latitude of the subradar point; when observations are confined to short periods around oppositions, decades are required for all points to have near mates\*. For

---

\*With the upgraded Arecibo radar facility, observations of useful accuracy will be obtainable nearly to superior conjunction. But because of the limitations on the angular motion of the feed, observations are only possible when Mars is at positive declinations.



Mercury and Venus, slow planetary rotation and the diurnal motion of the earth, as well as the slow drift in latitude of the subradar point make it difficult to obtain closure points. Furthermore, the nearly eight-year periodicity in the relative orbital motions of the earth and Venus, and the nearly thirteen-year periodicity in the corresponding motions of the earth and Mercury, tend to introduce "aliasing" effects in the determination of the planetary orbits from the closure points.

We must also emphasize the difficulty caused by increased measurement accuracy. Such improvements almost inevitably are accompanied by increased surface resolution which perforce makes more difficult the obtaining of closure points. This vicious cycle aspect of increased measurement accuracy is partially offset by the ability to measure delays, in one observation, to a fairly dense set of points along the (instantaneous) Doppler equator. One might have questioned the usefulness of this technique: Why not simply make determinations only at the subradar point where the signal-to-noise ratio is highest? The answer is clear: Use of this "Doppler-equator" technique greatly enhances the number of closure points that can be obtained.

It is, of course, not necessary that the topography be determined solely from ground-based observations. Altimeters aboard spacecraft, such as the Pioneer Venus Orbiter, can be used to obtain high-accuracy and high-resolution topographic information. These data and the radar data, where overlap exists, would serve to verify the accuracy of both techniques.

Finally, to place matters in perspective, we remark that, at present, the radar measurement residuals attributable to topography, after the removal of the low-frequency terms by use of the two-dimensional Fourier series, range from about 1 to 3  $\mu$ sec rms for the inner planets.

#### IV. Current Status and Prospects for Radar Tests of Relativity

In this final section of Part I, we give a brief summary of the current status of the radar tests of general relativity and of the prospects for improvement.

1. Retardation of Signal Propagation

From late in 1966 through the summer of 1971 attempts were made using the Haystack Observatory's X-band ( $\lambda \approx 3.8$  cm) radar system to detect the direct effect of solar gravity on interplanetary time delay measurements. The periods near the superior conjunctions of Mercury and Venus were especially useful for this purpose. Because of dwindling support for the radar system, its effectiveness slowly decreased with time. The combined analysis of these radar data yielded, through the parameterization given in Equation (2.2), a result:

$$\left(\frac{1+\gamma}{2}\right) \approx 1.00 \pm 0.04, \quad (4.1)$$

where the uncertainty quoted represents our best judgment as to the true standard error of the determination and is severalfold higher than the formal standard error based on setting the rms of the postfit residuals to unity. The last published result from this series of experiments,  $[(1+\gamma)/2] \approx 1.01 \pm 0.05$  (Shapiro et al., 1971b), was based on fewer radar data but is not substantially different from Equation (4.1). The main differences in the data sets were the additional time-delay data obtained near the superior conjunction of Venus in August and September 1971 and the extra data obtained near the preceding and following inferior conjunctions which allowed improvements

in the determination of the topography\*.

In Figure 3 are shown a sample of the postfit residuals for a typical solution involving the inner-planet radar time-delay data and the several hundred parameters needed to describe the orbits, masses, and topography of these planets as well as various other solar-system constants. The residuals are displayed relative to the "excess" delay given in Equation (2.2). Such a display is useful in that it shows at a glance the relative sizes of the residuals and the relativistic effect, but it is also somewhat misleading in that the "masking" effects due to the correlations of the estimate of  $\gamma$  with those of the other parameters is suppressed. One further point must be made in connection with the figure and the solution on which it is based: The errors assumed for the measurements had a minimum value of 3  $\mu$ sec, despite the fact that many of the time-delay observations, especially near the last two inferior conjunctions

---

\* Because of the apparent resonance between Venus' spin and the relative orbits of the earth and Venus, the same longitudes, although, in general, different latitudes, are observed at inferior and superior conjunctions.

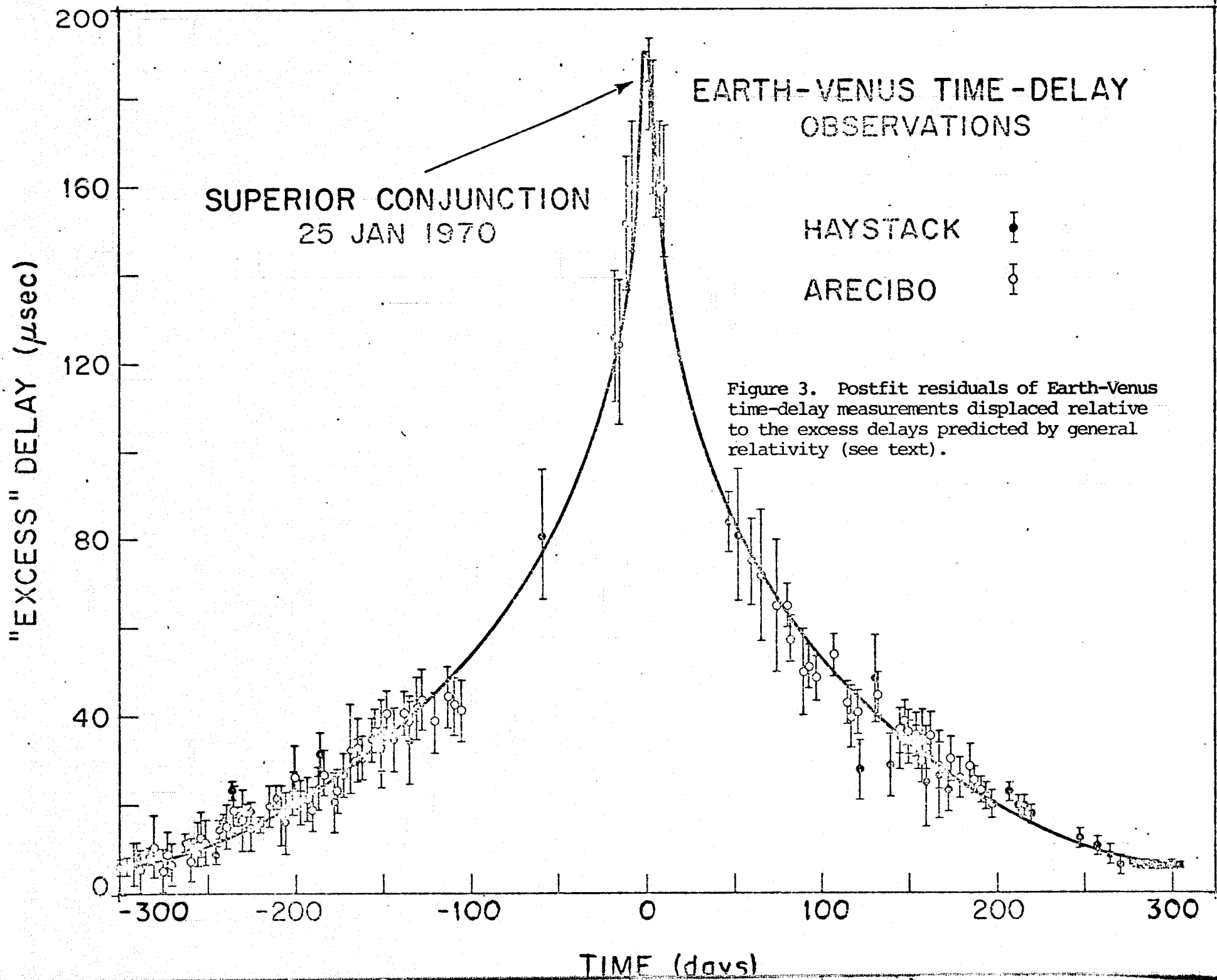


Figure 3. Postfit residuals of Earth-Venus time-delay measurements displaced relative to the excess delays predicted by general relativity (see text).

of Venus, had measurement uncertainties as low as a few tenths of a microsecond. The purpose of this ad hoc adjustment was to compensate partially for the failure to model the high-frequency components of the topography (see Section III. 6)\* Complementing this radar-alone result, the Mariner 9 ranging data, when combined with the radar data yielded a preliminary value for  $[(1+\gamma)/2]$  with only a 2% uncertainty. The analysis of these Mariner 9 data is being carried out collaboratively between JPL and MIT; however, certain small discrepancies still remain to be resolved before a value can be given confidently and the result submitted for publication.

In the future, at least an order of magnitude improvement in the radar-alone result for this experiment should be obtainable through simultaneous, or near simultaneous, S- and X-band observations of Mercury or Venus near

---

\*This particular solution did not take advantage of the correlations in the topography for near closure points, but this neglect has no appreciable effect on either the estimate of  $\gamma$  or its uncertainty: Too few closure points exist at present from the radar observations of Mercury and Venus.

superior conjunctions, using the newer, more sensitive radar systems. The upgraded Arecibo facility, however, will initially be equipped only at S-band; for this system the solar corona will probably limit the improvement obtainable to a factor of four or so, yielding about a 2% uncertainty in  $\gamma$ . If the improved antenna surface at Arecibo provides sufficient efficiency at X-band, then the desired two-frequency experiment could be conducted at Arecibo. Even if a high-power X-band transmitter were not available there, it would be possible to utilize the Haystack radar system for transmission of the X-band signals and Arecibo for reception, assuming, of course, that the latter can be equipped with a suitable receiver. Another possibility would be to use the 210-foot-diameter Goldstone radar which is now equipped with an X-band system to complement its S-band one. Given the ability to carry out dual-frequency measurements at Goldstone alone, or coordinated measurements at Arecibo (S-band) and Goldstone (X-band), the main limitation on the accuracy of this experiment will probably be set by the unmodelled parts of the topography on the target planets. Repetition would improve the accuracy but only slowly. Nevertheless, there appears to us little reason to doubt that the uncertainty in  $\gamma$  can be driven substantially below 1% through these radar measurements, at least down to 0.6%.

In fact, the radar versions of this important experiment \* might outperform the spacecraft versions over the next

few years. Several circumstances could lead to this result: First, presently planned spacecraft involve ranging on two frequencies at most only on the downlink from the spacecraft to the ground receiver; the uplink is limited to S-band. Thus, depending on the spectra of the temporal and spatial variations of the coronal electron densities, it may not be possible to correct adequately for the coronal effects on the uplink part of the delay measurement. Second, nongravitational forces or, in the case of orbiters, unmodelled parts of the planet's gravity field, could limit the interpretation of the earth-spacecraft delay measurements and, hence, the accuracy of the estimate of  $\gamma^*$ . It is simply not possible on the basis of present knowledge to predict reliably whether the passive or active version of the "excess" delay experiment will yield the higher accuracy in the next few years.

---

\*Landers could eliminate this problem, but the only ones currently planned -- for Viking -- have only an S-band capability and ranging to them will be severely limited by other constraints on the mission.



## 2. Advances of Planetary Perihelia

The accurate determination of the advances in planetary perihelia attributable to relativistic effects is made difficult by the lack of an accurate, independent determination of the solar gravitational quadrupole moment as discussed in Section III.4.iii.

To the extent that the parameter  $J_{2\odot}$  that characterizes the solar quadrupole moment can be neglected in its influence on planetary orbits, we can obtain a very precise measure of the relativistic contributions to the perihelion advances. As shown by Shapiro et al. (1972b), the radar data through 1971 implied

$$\frac{2+2\gamma-\beta}{3} = 1.00_5 \pm 0.02 \quad (4.2)$$

for the coefficient of the secular advance as given in Equation (2.3). The accuracy of this result relied primarily on the radar observations of Mercury. Estimates of a separate parameter for the secular advance of each of the inner planets showed that only for Mercury was the uncertainty under 0.1.

With the larger set of inner-planet radar data now available, we have estimated the relativistic parameters simultaneously with  $J_{2\odot}$  and the other relevant parameters described in the previous subsection. The preliminary

results indicate that

$$\left(\frac{2+2\gamma-\beta}{3}\right) = 0.98 \pm 0.04 \quad (4.3)$$

and

$$J_{2\odot} = (0.5 \pm 1.5) \times 10^{-5}. \quad (4.4)$$

However, because of the unusually strong correlation ( $\approx 0.99$ ) between these parameters, the results are very susceptible to significant distortion by systematic errors. The exposure of the effects on these results of any such systematic errors present in either the data or the theoretical model, especially of the topography, requires a painstaking series of sensitivity studies. In particular, the parameter estimates and the postfit residuals must be obtained for reasonably wide variations in error weightings, in models of the topography, etc. The results given in Equations (4.3) and (4.4) are based on a set of such studies that we regard as only partially complete; therefore no firm reliance can yet be placed on the numbers given; they are truly preliminary.

We expect to obtain substantial improvements in these results not only from the continued collection of radar data which perforce extend the time base, but, perhaps, more importantly, also from the development of a much larger set of near-closure points. The method of determination of topography along an arc of the Doppler equator with each observation, described in Section III. 6, has proven very

fruitful due to the increase in radar system sensitivity recently achieved at both Arecibo and at Goldstone\*. Examples of the topography of Venus determined by this method at Arecibo and at Haystack are shown in Figures 4 and 5, (Campbell et al., 1975). Similar results for Mercury obtained at Goldstone have been published by Goldstein and Zohar (1974); however, these Goldstone delineations of the topography were adjusted so that the values for each day have a zero mean and a zero net slope. In this form they cannot be used to the same full advantage for the purposes of the radar tests of relativity as can the Arecibo and Haystack results. More complete coverage, with "overlap" of the arcs from different days of observation, as obtained at Arecibo and Haystack, will enable the Goldstone data -- both past and future -- to be of full use.

The relatively favorable 1973 opposition of Mars provided an extended opportunity at Arecibo, Goldstone, and Haystack to obtain detailed and dense topographic coverage of that planet. In Figure 6 we present a small segment of a topographic contour which illustrates that the terrain over certain parts of the surface can be extraordinarily flat. Such parts are, of

---

\*The improvement referred to here for Arecibo relates primarily to a new feed obtained 2 years ago which yielded an increase in radar sensitivity of about 7 db. At Goldstone, the improvement was due to the installation of a 400 kw transmitter on the 210-foot-diameter (DSS14) antenna.

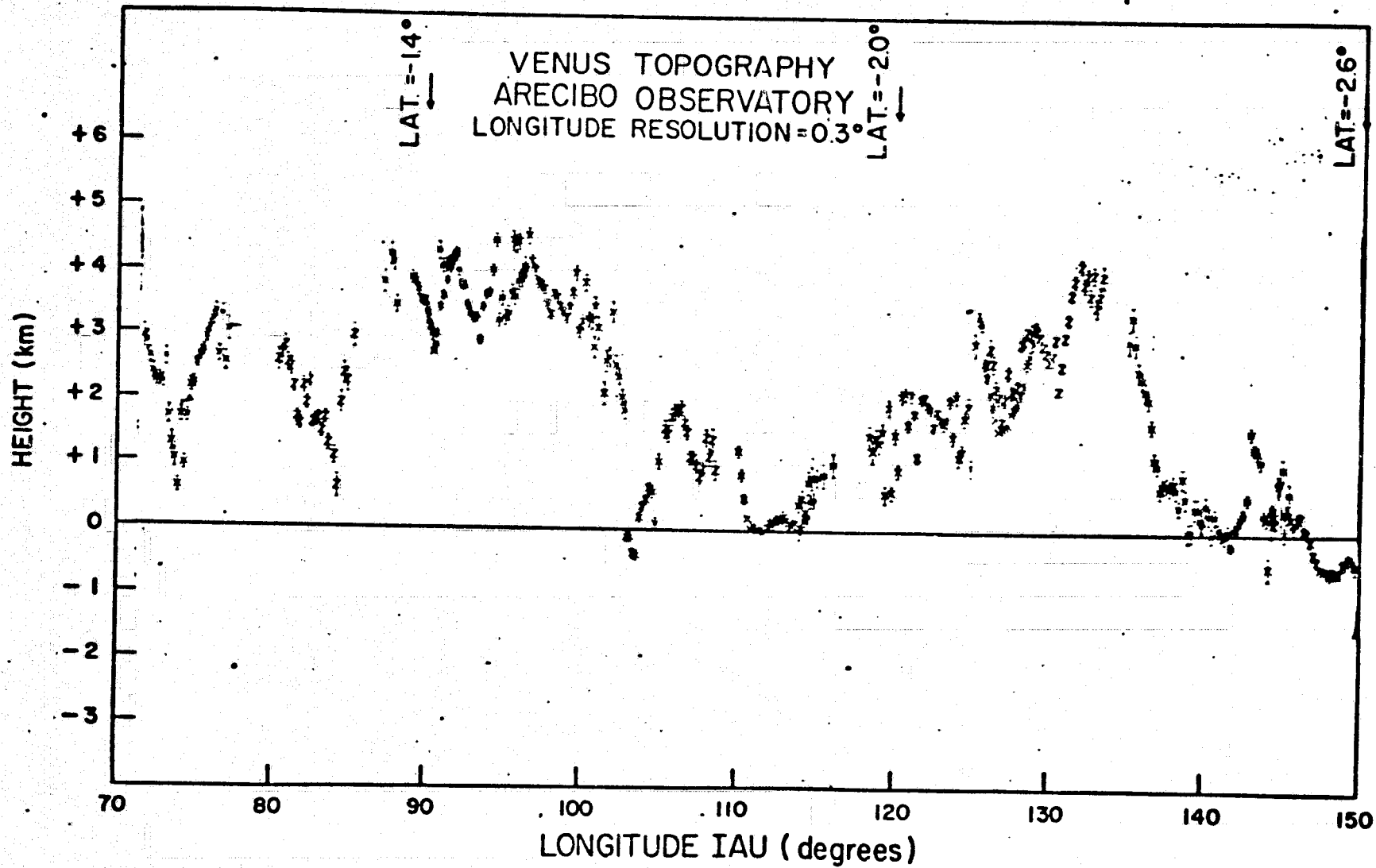


Figure 4. Topography along a section of the Doppler equator on Venus determined from radar observations carried out at the Arecibo Observatory.

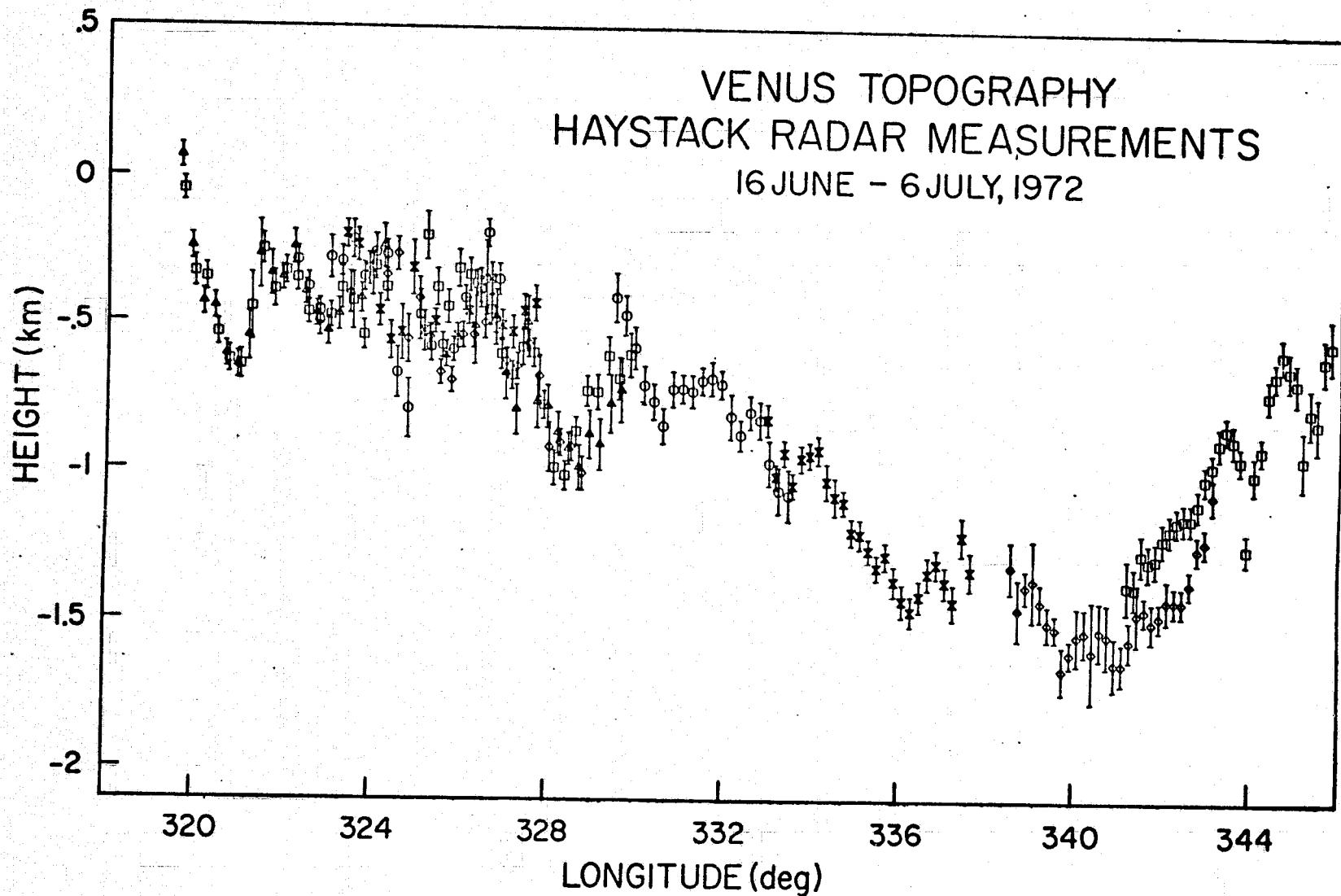


Figure 5. Topography along a section of the Doppler equator on Venus determined from radar observations carried out at the Haystack Observatory. The longitudes are as defined by the IAU.

# MARS TOPOGRAPHY

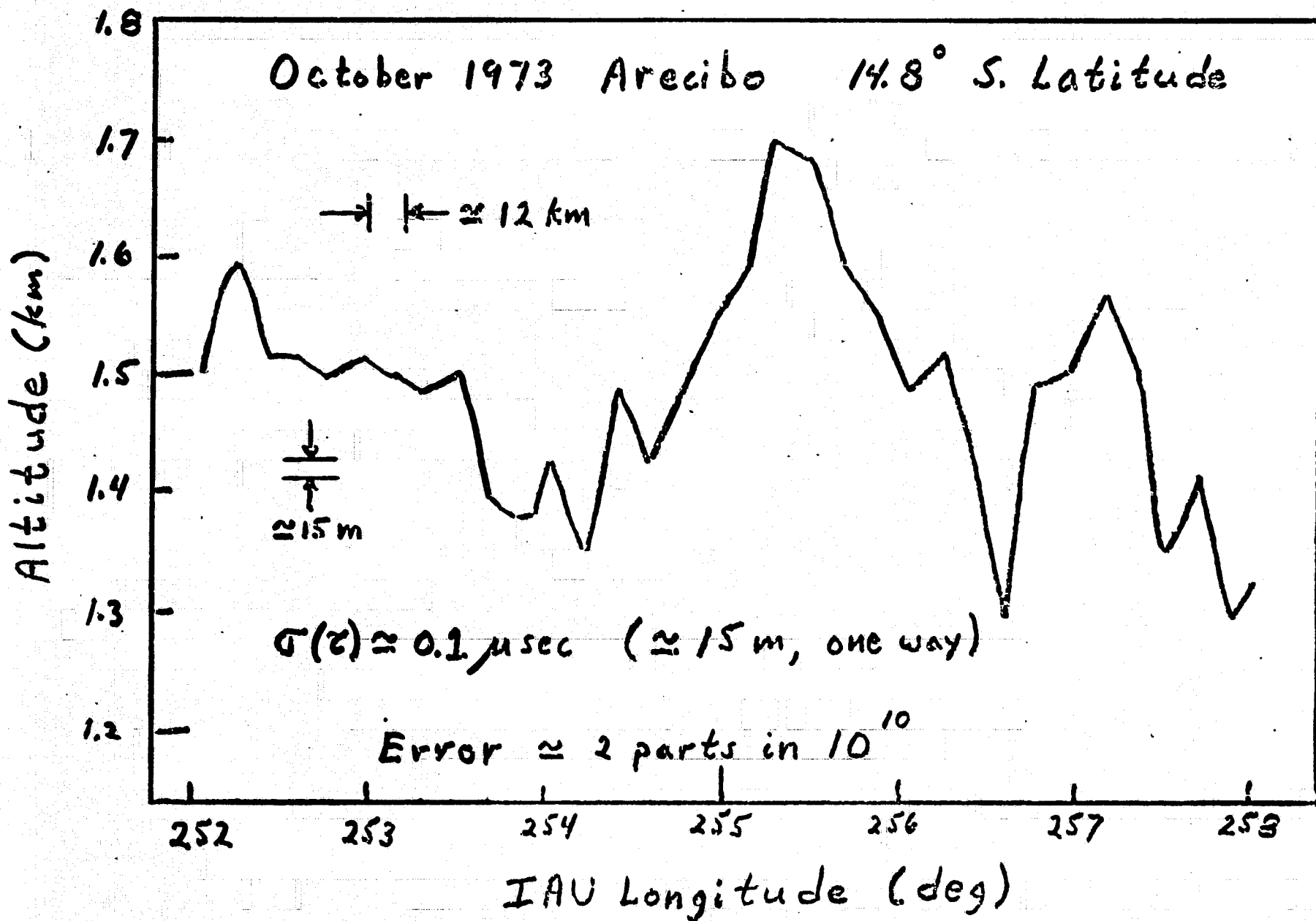


Figure 6. Topography along a short arc on the surface of Mars determined from radar observations carried out at the Arecibo Observatory.

course, highly suitable for the relativity tests since the correlation between near closure points can be reliably determined and the most effective use thereby made of the data for orbit analysis. Parts of the surface characterized by smooth, gentle undulations are almost as useful.

We must also call attention to the order of magnitude difference in the uncertainties in Figure 6 as compared to those in Figures 4 and 5. Because of the high signal-to-noise ratios achievable with the Mars observations, the uncertainties in many of the time-delay measurements were at, and sometimes below, the 0.2  $\mu$ sec level. With use of the upgraded Arecibo radar system, such accuracies will be achievable in time-delay measurements over major fractions of the geocentric orbits of Mercury, Venus, and Mars, and not simply in the immediate vicinities of close approaches. The limitation on the interpretation of the data for tests of relativity may then be set by the interplanetary plasma unless X-band or dual-frequency observations are made (see Section III. 3. iii).

In gathering new data, attention must of course be directed towards securing as many "mates" as possible to form closure points with past data. In this manner the value of past data for tests of relativity can be increased commensurate with the intrinsic measurement accuracy achieved. Such attention was devoted in the 1973 Mars

observations and, as a result, many near closure pairs and triplets were formed with observations from the 1971 Mars opposition. Errors for each element of a pair in many cases were below 0.3  $\mu$ sec. Although these data have not yet been fully analyzed one can safely conclude that the useful accuracy of these pairs for orbit determination will be at least at the 0.5  $\mu$ sec level. This conclusion stands in marked contrast to the ESRO (1974) statement that the distance from the earth to the center of mass of a target planet could not be obtained by radar ranging to even 1 km which is equivalent to an uncertainty greater than 6  $\mu$ sec in round-trip time delay -- a limit more than tenfold poorer than that given above.

To focus the above discussion on closure points and topography in their likely implications for improvement in the radar determinations of  $J_{2\odot}$  and the relativistic contributions to perihelia advances, we draw the following conclusion: If a vigorous program for radar observations of the inner planets is sustained at Arecibo over the next lustrum, the uncertainties in the determinations of  $J_{2\odot}$  and the combination  $(2+2\gamma-\beta)$  -- without the application of any a priori constraints based on other estimates -- should be reliably bounded by

$$\sigma(J_{2\odot}) < 3 \times 10^{-6} \tag{4.5}$$

$$\sigma\left(\frac{2+2\gamma-\beta}{3}\right) < 1 \times 10^{-2} \tag{4.6}$$

Sufficient redundancy should be available in the coverage of that part of the surface spanned by the subradar points on each planet that topography need not be the limiting



factor in accuracy. The interplanetary medium would probably set the limit. With dual-frequency or X-band observations being available routinely, the limitation would be set by the capabilities of the timing system and of the effective pulse lengths planned for use initially with the upgraded Arecibo radar. Improvements in these aspects, which are not yet constrained by the state-of-the-art, would then complete the circle by once again placing the accuracy limit on topography.

We have ignored the possible contributions of Goldstone in the above discussion primarily because of its lack of availability for sustained observations, due to the demands for spacecraft tracking. Although it is true that the sensitivity of the Goldstone radar system will be about an order of magnitude or so lower than Arecibo's, one has a long way to go before system sensitivity will place the primary limit on the accuracy of most of these tests of relativity. Therefore even limited observations at Goldstone could be very useful, especially if occasionally coordinated with Arecibo's to provide valuable independent checks on possible timing errors, etc.\* It is rarely, if ever, a good policy to rely solely on one instrument for an important experiment.

Finally, we emphasize that the bounds presented in Equations (4.5) and (4.6) are felt to be realistic but not particularly conservative. Although covariance analyses

---

\*The Haystack Observatory is no longer supported for radar observations of the planets and so cannot contribute to such checks.

performed by us indicate that substantially better accuracies can be achieved, we know from experience that unaccounted for systematic errors invariably degrade the results.

### 3. Variation of the Gravitational Constant

The analysis primarily of five years of earth-Mercury radar observations yielded an upper bound (Shapiro et al., 1971a) on the possible time variation of the gravitational constant of

$$\left| \frac{\dot{G}}{G} \right| < 4 \times 10^{-10} \text{ yr}^{-1}. \quad (4.7)$$

Data accumulated over the past three years, combined with the earlier data, have been undergoing analyses similar to those described above in connection with the perihelia advances. In fact many of the sensitivity studies are identical as they serve both purposes; in others for  $\dot{G}$ , for example, the parameters  $\gamma$  and  $\beta$  are set to unity or to the Dicke (1974) values 0.89 and 1.00, respectively. Preliminary results from these recent, but as yet incomplete, sensitivity analyses yield

$$\left| \frac{\dot{G}}{G} \right| < 10^{-10} \text{ yr}^{-1}. \quad (4.8)$$

Again we must point out that this bound is subject to the same caveats as were mentioned in connection with Equations (4.5) and (4.6). The result on the signal retardation, given in Equation (4.1), is largely exempt

from these difficulties for two reasons: (1) the time-delay effect has a unique, logarithmic signature; and (2) the accuracy is limited mostly by the errors in the measurements made near superior conjunction where the effect is a maximum and the signal-to-noise ratio a minimum.

To return to the discussion of Equation (4.8), we note that the fourfold improvement in this bound compared to Equation (4.7) is due to several factors: (1) the increased time span of the data; (2) the improved accuracy of the measurements; (3) the incorporation of a model for the low-frequency components of the topography; and (4) the accurate, independent determination of the mass of Mercury. Until recently, the estimate of the mass of Mercury was dependent on the radar data and was fairly well correlated (coefficient  $\approx 0.5$ ) with the estimate of  $\dot{G}$  (Shapiro et al., 1971a). The Mariner 10 flyby of Mercury provided a more accurate, independent determination (Howard et al., 1974):

$$M_{\oplus}^{-1} = 6,023,600 \pm 600, \quad (4.9)$$

where  $M_{\oplus}$  is the mass of Mercury in units of the sun's mass. This result for Mercury's mass is in embarrassingly good agreement with our prior publications of determinations based on analysis of radar data [viz.  $M_{\oplus}^{-1} = 6,022,000 \pm 53,000$  (Ash et al., 1967);  $M_{\oplus}^{-1} = 6,025,000 \pm 15,000$  (Ash et al., 1971); and  $M_{\oplus}^{-1} = 6,022,900 \pm 900$  (Shapiro and Reasenberg, 1973)] and shows that our earlier result, as distinct from its uncertainty, was not adversely affected by the need to estimate  $M_{\oplus}$  simultaneously with  $\dot{G}$ .

As for the future, improvements in the estimate of  $\dot{G}$  depend on the same factors addressed in the previous subsection. The same assumptions that yielded the bounds given in Equations (4.5) and (4.6) also imply

$$\sigma\left(\frac{\dot{G}}{G}\right) < 2 \times 10^{-11} \text{ yr}^{-1} \quad (4.10)$$

as a reliable bound that could be achieved by the early 1980's.

#### 4. Principle of Equivalence

There has not yet been any radar test of the Principle of Equivalence in regard to the relative contribution of the gravitational binding energy of solar-system bodies to their respective inertial and gravitational masses. With present technology, the only other possible test of this contribution is from laser ranging to the retroreflectors on the moon, as mentioned in Section III.6. Radar appears to offer a significant test through the measurements of time delays of signals propagating between the earth and the other inner planets. In this test each of the inner planets acts like a small particle moving within the Jupiter-sun system, and, therefore, the measurements must extend in time over a number of orbital periods of the relevant inner planets to obtain an accurate result. By the early 1980's the relative contribution of the gravitational binding energy should be

determined to within a few percent if a vigorous program of radar measurements is pursued throughout the intervening years. Significantly higher accuracy, comparable to that attainable from lunar laser ranging, will be achievable if ranging data for spacecraft in planetary orbits are also obtained. The best opportunities will be afforded by the Viking Mission to Mars and the Pioneer Venus Orbiter. Ranging data for the spacecraft involved in these missions could not only be of higher quality in their own right, but would provide unique opportunities to calibrate the radar measurements to these planets in terms of equivalent center-of-mass to center-of-mass delays. Independent checks of this type are very important and, in fact, enhance the value of both the spacecraft and the radar ranging data.

To summarize, it is our judgment that the continuation of interplanetary radar measurements on a regular basis, especially if carried out with the equipment improvements suggested above for the Arecibo facility, will yield substantial improvements -- from a factor of four to a factor of at least 10 -- in each of the gravitation tests discussed in this section. In each case, except for the signal retardation and Principle of Equivalence tests, the ground-based results depend vitally on observations of Mercury and therefore will outperform any likely to result from spacecraft at

least through the end of this decade. The combination of the spacecraft and the radar data, of course, offers the highest potential.

Further in the future one might anticipate accuracies sufficient to measure the next higher-order relativistic effects, but these might well require laser surveying of the solar system.

V. References

- Allen, C. W. 1963, Astrophysical Quantities (Athlone Press, London).
- Ash, M. E., W. B. Smith, and I. I. Shapiro 1971, Science 174, 551.
- Ash, M. E., W. B. Smith, and I. I. Shapiro 1967, Astron. J. 72, 338.
- Braginski, V. B. and V. I. Panov 1971, Zurn. Eksp. Teor. Fiz. 61, 875.
- Campbell, D. B. et al. (5 authors) 1975, in preparation.
- Clayton, D. D. 1968, Principles of Stellar Evolution and Nucleosynthesis (McGraw-Hill, New York).
- Colombo, G. and I. I. Shapiro 1966, Ap. J. 145, 296.
- Counselman, C. C. 1968, Ph.D. Thesis, Massachusetts Institute of Technology.
- Counselman, C. C., H. F. Hinteregger, and I. I. Shapiro 1972, Science 178, 607.
- Counselman, C. C. and J. M. Rankin 1972, Ap. J. 175, 843.
- Dicke, R. H. 1974, Science 184, 419.
- Dicke, R. H. and H. M. Goldenberg 1967, Phys. Rev. Lett. 18, 313.
- Duxbury, T. C. 1974, Icarus 23, 290.
- Dwight, H. B. 1949, Tables of Integrals and Other Mathematical Data (Macmillan, New York).
- Eddington, A. S. 1960, The Mathematical Theory of Relativity, (Cambridge University Press, Cambridge), p. 105.
- ESRO 1974, report on "Sorel" Mission.
- Evans, J. V. and T. Hagfors 1968, Radar Astronomy (McGraw-Hill, New York).
- Friedman, L. D. 1970, Ph.D. Thesis, Massachusetts Institute of Technology.
- Goldreich, P. and S. J. Peale 1966, Astron. J. 71, 425.

- Goldstein, R. M., and S. Zohar 1974, *Astron. J.* 79, 85.
- Goldstein, R. M. 1975, private communication.
- Hill, H. A. et al. (7 authors) 1974, *Phys. Rev. Lett.* 33, 1497.
- Howard, H. T. et al. (20 authors) 1974, *Science* 183, 1297.
- Howard, H. T. et al. (21 authors) 1974, *Science* 185, 179.
- Kliore, A. J. et al. (5 authors) 1972, *Science* 175, 313.
- Lense, J. and H. Thirring 1918, *Phys. Zeitschr.* 19, 156.
- Marsden, B. G. 1974, private communication.
- Matson, D. 1971, Ph.D. Thesis, California Institute of Technology.
- Miller, L. H. 1971, B. Sc. Thesis, Massachusetts Institute of Technology.
- Misner, C. W., K. S. Thorne, and J. A. Wheeler 1973, Gravitation (W. H. Freeman, San Francisco).
- Nordtvedt, K. 1968, *Phys. Rev.* 170, 1168.
- Pettengill, G. H. 1970, in Radar Handbook, ed. M. Skolnick (McGraw-Hill, New York).
- Robertson, H. P. 1937, *Mon. Not. Roy. Astron. Soc.* 97, 423.
- Robertson, H. P. 1962, in Space Age Astronomy, eds. A. J. Deutsch and W. B. Klemperer (Academic Press, New York), p. 228.
- Schubart, J. 1974, *Astron. & Astrophys.* 39, 147.
- Seidemann, P. K., W. J. Klepczynski, R. L. Duncombe, and E. S. Jackson 1971, *Astron. J.* 76, 488.
- Shapiro, I. I. 1964, *Phys. Rev. Lett.* 13, 789.
- Shapiro, I. I. 1966, *Phys. Rev.* 145, 1005.
- Shapiro, I. I. 1967, *Science* 157, 806.
- Shapiro, I. I. et al. (5 authors) 1971a, *Phys. Rev. Lett.* 26, 27.
- Shapiro, I. I. et al. (8 authors) 1971b, *Phys. Rev. Lett.* 26, 1132.
- Shapiro, I. I. 1972, *Gen. Rel. Grav. J.* 3, 135.
- Shapiro, I. I. et al. (5 authors) 1972a, *Science* 178, 939.



- Shapiro, I. I. et al. (6 authors) 1972b, Phys. Rev. Lett. 28, 1597.
- Shapiro, I. I. and R. D. Reasenberg 1973, in Jet Propulsion Laboratory Technical Report, No. 32-1550, 4, 453.
- Shapiro, I. I. 1973, Ann. N.Y. Acad. Sci. 224, 31.
- Shapiro, I. I. et al. (5 authors) 1974, Science 179, 473.
- Shapiro, I. I. et al. (11 authors) 1974, Science 186, 920.
- Sherman, G. N. 1973, Ph.D. Thesis, Massachusetts Institute of Technology.
- Sinclair, A.C.E., J. P. Basart, D. Buhl, and W. A. Gale 1972, Ap. J. 175, 555.
- Slade, M. A. 1971, Ph.D. Thesis, Massachusetts Institute of Technology.
- Tausner, M. J. 1966, Lincoln Laboratory Technical Report, No. 425.
- Van Flandern, T. C. 1975, Bull. Amer. Phys. Soc. Series II, 20, 543.
- Weinberg, S. 1972, Gravitation and Cosmology (John Wiley and Sons, New York).
- Weisberg, J. M., J. M. Rankin, R. R. Payne, and C. C. Counselman, to be submitted to Ap. J.
- Will, C. M. 1973, in Experimental Gravitation, ed. B. Bertotti (Academic Press, New York), p. 1.
- Zisk, S. H. 1972, Science 178, 977.

Part II

Radio-Interferometric Measurement of the Solar Gravitational  
Deflection of Radio Waves

I. Introduction

A resurgence of interest in the measurement of the gravitational deflection of "light" rays by the sun has followed the realization (Shapiro, 1967) that radio interferometry could be gainfully employed for the purpose (Seielstad et al., 1970; Muhleman et al., 1970; Sramek, 1971; Hill, 1971; Sramek, 1972; Riley, 1973; Weiler et al., 1974). Here we describe in some detail the method of very-long-baseline interferometry (VLBI) that we have recently used to obtain a very accurate result for the deflection experiment (Counselman et al., 1974). The previously published results which all involved short-baseline, or, more precisely, connected-element, interferometry were of lower accuracy;\* an extended discussion of these short-baseline-interferometry techniques was given by Sramek (1973).

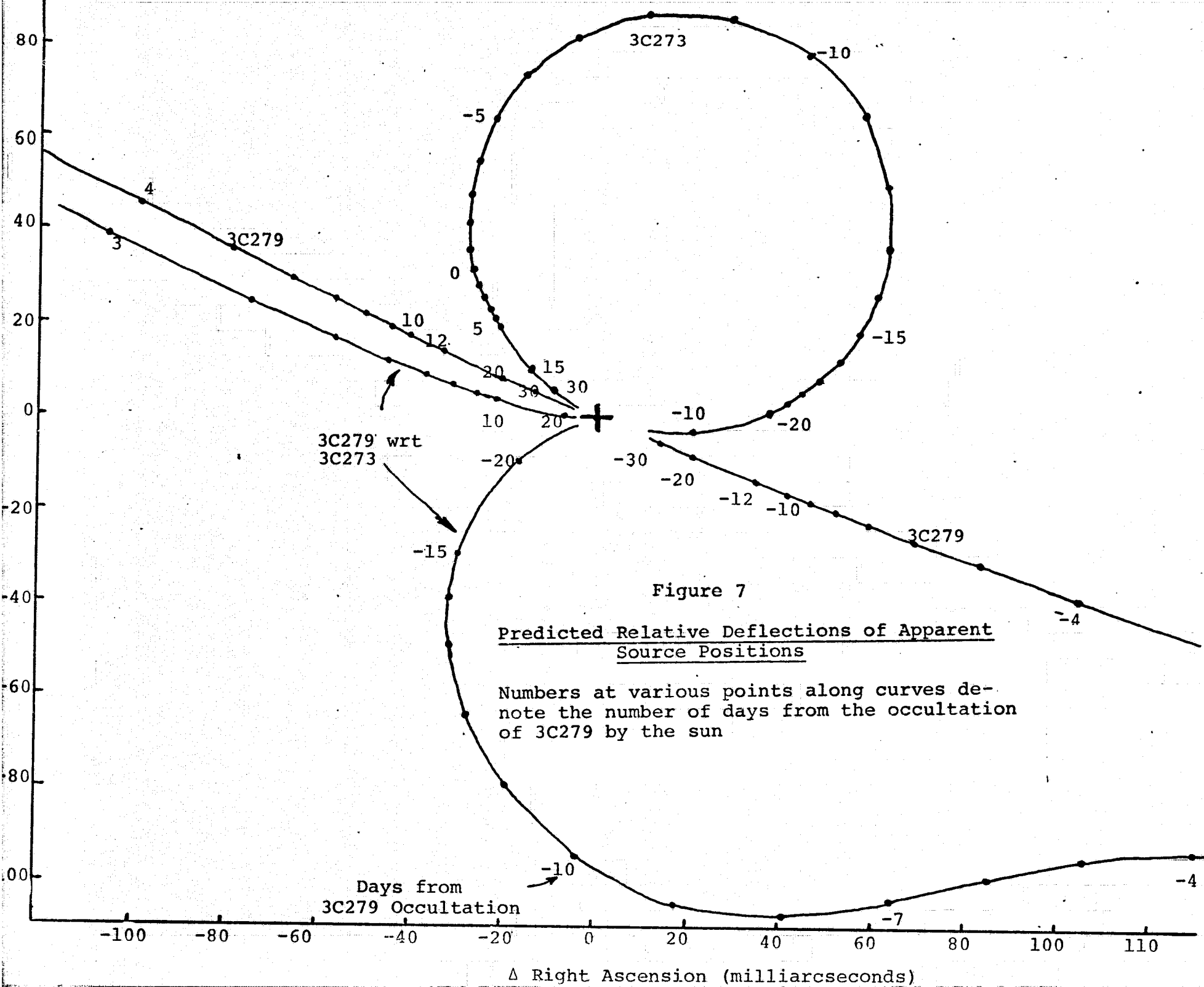
In our experiment, carried out in the fall of 1972 at a radio frequency of 8105 MHz ( $\lambda \approx 3.7$  cm), we utilized the 120-ft and the 60-ft-diameter antennas of the Haystack Observatory in Tyngsboro, Massachusetts (the "Haystack" and the "Westford" antennas), and two 85-ft-diameter antennas of the National Radio Astronomy Observatory (NRAO) in Green Bank, West Virginia, some 845 km to the southwest. Haystack and one NRAO antenna formed a long-baseline interferometer, and both these antennas were directed at the compact extragalactic radio source 3C279. Westford and

---

\* Recently a "long" short-baseline experiment was performed which yielded somewhat higher accuracy (Fomalont and Sramek, 1975).

the other NRAO antenna formed another long-baseline interferometer and were directed at a similar source, 3C273B, located about  $10^\circ$  to the northwest of 3C279. On 8 October, 3C279 was occulted by the sun. By observing 3C273B simultaneously we were able to make relative measurements between the two sources, to prevent the introduction of errors by the separate frequency standards employed at Haystack and NRAO to govern the heterodyning and recording of the signals at the two sites. (The two antenna-receiver systems at a given site both utilized the same frequency standard.) Removal of effects of the differences between the frequency standards was accomplished by taking as the basic observable the difference between the interferometric fringe phases determined for 3C279 and 3C273B. The use of this difference observable also served to reduce the effects of the neutral atmosphere and ionosphere.

The use of this difference fringe-phase, or DFP observable also reduces the sensitivity to the gravitational deflection. The amount of the reduction is shown in Figure 7 as a function of time. The gravitational deflection can be detected only by determining the change in the apparent relative positions of the two sources during the period



surrounding the occultation on 8 October. Both the right-ascension and the declination differences between the sources are changed by the gravitational deflection.

However, because 3C273B and 3C279 both lie near the celestial equator, the DFP observable is sensitive mainly to their right-ascension difference. If, for the purpose of explanation, we neglect the solar corona, the ionosphere, the atmosphere, aberration, and numerous other small effects, we may express the DFP,  $\Delta\phi$ , approximately as a function of the right-ascension difference,  $\Delta\alpha$ , between the sources as

$$\Delta\phi \approx \frac{2\pi B}{\lambda} \cdot \Delta\alpha \cdot \cos H + \Delta\phi_0 \quad (\text{modulo } 2\pi) \quad (1.1)$$

in which B is the length of the equatorial projection of the long baseline vector,  $\lambda$  is the wavelength, and H is the hour angle at the midpoint of the baseline of a point midway between the sources. The quantity  $\Delta\phi_0$  is a constant which depends on the baseline and the declinations of the sources but which, most importantly, includes the unknown constant difference between the phases of the independent local oscillators of the receiving stations. Because  $\Delta\phi_0$  is normally unknown, it is necessary to observe  $\Delta\phi$  continuously through a range of hour angle H during which  $\cos H$  varies significantly, preferably near the times of rise ( $H \approx -6^h$ ) or

set ( $H \approx +6^h$ ), in order to determine  $\Delta\alpha$ .\* If the change of  $\Delta\phi$  between the time of rise (or set) and transit can be measured with an uncertainty of  $\sigma_\phi$ , it follows that the uncertainty of the estimate of  $\Delta\alpha$  is approximately

$$\sigma_{\Delta\alpha} \approx \frac{\lambda}{2\pi B} \sigma_\phi. \quad (1.2)$$

The determination of the DFP during each day of observation without the introduction of any  $2\pi$  ambiguities, aside from any contained in the constant,  $\Delta\phi_0$  term in Eq. (1.1), is a crucial requirement of the experiment. That is, the constant  $\Delta\phi_0$  must be the same for all measurements throughout a day's observations. Because the DFP is intrinsically an ambiguous observable, no large gaps in its determination as a function of time can be tolerated. In particular, for a gap to be "acceptable", one must be able to connect the measurements of DFP before and after the gap without the introduction of any  $2\pi$  ambiguity. During observations when the ray path to 3C279 passes within a few degrees of the sun, a gap of only a few seconds may be

---

\* Atmospheric phase delay increases abruptly near the times of rising and setting. In order to separate  $\Delta\alpha$  from atmospheric parameters, the observation interval must be extended a few hours from rise or set. Note that a determination of  $\Delta\alpha$  may be made from observations entirely before transit, and another, nearly independent, determination may be made after transit on the same day.

unacceptable, because the solar corona introduces rapid and unpredictable variations in the fringe phase. On the other hand, when the separation of sun and source is  $10^\circ$  or more, even a gap of 30 min may be successfully bridged, as demonstrated below.

One might wonder why the time-derivative of the differenced fringe phase, the so-called differenced fringe rate, or DFR, is not used as the basic observable since it is intrinsically unambiguous. A simple calculation shows that the ratio of the errors in the determination of the relative right ascensions,  $\Delta\alpha$ , for the two sources via the two methods is given by

$$\frac{\sigma_{\Delta\alpha}(\text{DFP})}{\sigma_{\Delta\alpha}(\text{DFR})} \approx \Omega T, \quad (1.3)$$

where  $\Omega \approx 2\pi/\text{day}$  is the rotational angular velocity of the earth and  $T$  is the integration time used to determine a value for the DFR. If this time is very short relative to a day, the accuracy achievable with the DFR observable may be orders of magnitude less than with the DFP, all other aspects of the experiment being equal.

## II. Observations

The main characteristics of the antenna-receiver systems used in our experiment are described in Table 3.

Table 3

Characteristics of Four-Antenna Interferometer

Radio telescope	Location	Effective aperture (m <sup>2</sup> )	System temperature (K)	Observed source
Haystack*	Tyngsboro, Mass.	480	80	3C279
Westford*	Westford, Mass.	120	250	3C273B
85-2†	Green Bank, West Virginia	240	240**	3C273B
85-3†	Green Bank, West Virginia	240	240**	3C279

---

\* Operated by the Haystack Observatory.

† Operated by the National Radio Astronomy Observatory (NRAO).

\*\* Single side band.



Local-oscillator signals for both systems at a given end of the long baseline were derived from the same frequency standard. At the Massachusetts end, the 5 MHz signal from a hydrogen-maser frequency standard located at Haystack was multiplied to approximately 130 MHz and the resulting power split, one portion being sent to Westford over a cable whose electrical length was continuously servo-controlled. Although the remainder of the frequency-multiplication chain at Westford was independent of that at Haystack, this additional multiplication should not have introduced a significant difference between the phases of the local oscillators of the two antennas. At Green Bank, the signal from the hydrogen-maser frequency standard was carried to the two antennas by buried cables. The detailed setup at Green Bank was essentially identical with the usual one employed when these two antennas form a short-baseline interferometer, for which the phase-stability requirements are far more stringent than for our experiment. The signals received from each source were converted from microwave to low frequencies, then clipped (only the sign was preserved), sampled, and recorded digitally at a rate of 720 kb/sec on magnetic tape using the NRAO Mark I system (Bare et al. 1967). On each tape alternate records, of duration 0.2 sec, were used for a given source, so that the recorded signals from the two sources were interleaved. Four tape recorders

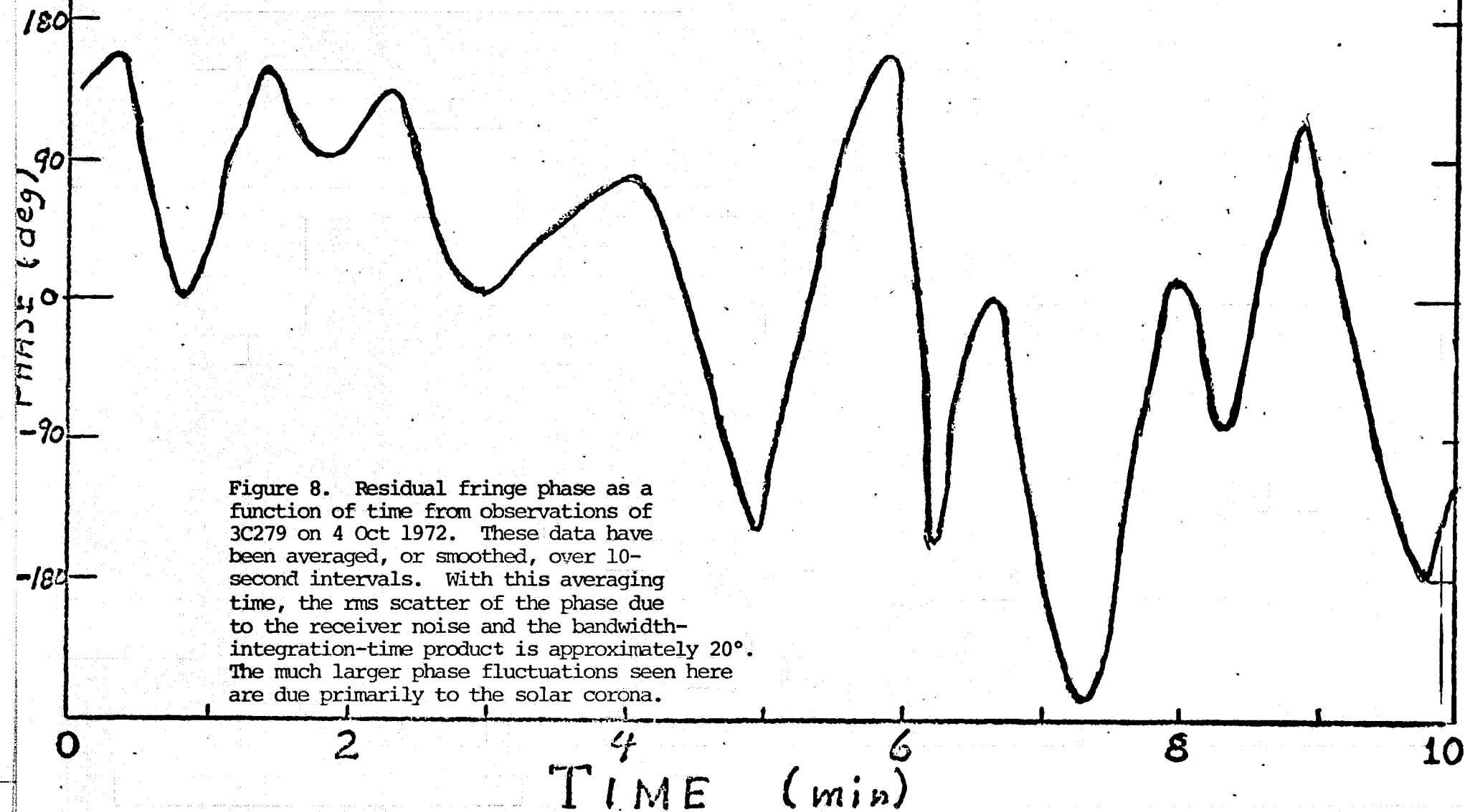
were used at each site, in order to obtain uninterrupted recording: two on line at any given time with one recording and one rewinding, and two spares. These latter were needed often, because the mean-time-between-failures of a recorder was only a few hours. Maintaining uninterrupted recordings for nine hours of observation each day, with each separate tape holding only three minutes of data, required unusual devotion of the operating personnel. All told, about 5000 magnetic tapes were utilized, containing a total of about 3600 kilometers of tape and about  $7 \times 10^{11}$  bits of data.

These data were all processed at the Haystack Observatory with a special-purpose digital correlator connected to the Observatory's CDC 3300 computer. The combination allowed a tape pair to be processed in about four minutes, the output being the fringe amplitude and phase for each 0.2-sec record; the output was then averaged coherently over longer intervals. Although a variety of different averaging intervals was used in the course of the analysis, the typical procedure was to form 10-sec averages and, from these, the DFP observable. A simple computer program was used to connect the sequence of values of the DFP without the introduction of spurious  $2\pi$  changes. However, because of

the subtlety of the process, we examined every single phase connection graphically to insure its validity; in every doubtful case, we re-examined the connection with successively smaller averaging intervals for the DFP until either the reliability of the connection could be assured or the statistical uncertainty in the determination of the fringe phase became too high to allow a reliable connection. This latter stage was reached for an averaging interval of about 1 sec. In such cases we assumed the connection to be broken and we introduced a new unknown constant [See Eq. (1.1)] at the appropriate epoch into the theoretical model for the DFP observable. Figure 8 shows the behavior of the fringe phase for 3C279 for a short span of time on 4 October. This sample of data illustrates the obstacles to reliable phase connection introduced by data gaps and the solar corona.

It is worth noting that the amount of turbulence in the solar corona in the relevant range of spatial scales (i.e., those not large compared to the Haystack-NRAO baseline) was exceedingly time-variable; for example, the DFP was very smooth for the first few hours of observation on 3 October and then, within less than 5 minutes, the DFP became impossible to follow with 1-second averaging.

4 OCTOBER 1972



Such severe coronal fluctuations caused us to eliminate as worthless some segments of the data. In addition, segments within which the phase connection was reliable, but which were shorter than about an hour, added no useful sensitivity to the determination of the relative position of the sources and were not utilized.

After completion of this phase-connection and editing process, the DFP data were smoothed by straight-line fitting over 3-minute intervals corresponding to the duration of the original tape recordings to obtain one datum every 3 minutes (except, of course, where the original data had contained gaps). All of the resulting data, from 23 and 25 September, 1, 2, 3, 4, 10, 11, 13, 18, 19, and 20 October 1972, were combined in the final analysis.

### III. Analysis

In this analysis we assumed that the apparent solar gravitational deflection of the position of a source was given, in radians, by (Shapiro, 1967)

$$(2 + 2\gamma) \frac{GM_{\odot}}{c^2 p}, \quad (3.1)$$

where  $\gamma$  is the unknown parameter to be estimated (general relativity predicts the value  $\gamma = 1$ );  $G$  is the

gravitational constant;  $M_{\odot}$  is the mass of the sun;  $c$  is the speed of light; and

$$p = 2r \tan (\theta/2), \quad (3.2)$$

where  $r$  is the distance from the observer to the center of mass of the sun and  $\theta$  is the angle subtended at the observer, between the source and the center of the sun. The value of  $\gamma$  and the undeflected position of 3C279 relative to that of 3C273B were estimated simultaneously with a large set of other unknown parameters by means of iterative least-squares adjustment. These unknowns included the  $\Delta\phi_{\odot}$  constants [Eq. (1.1)] and atmospheric-model parameters, as discussed below.

The undeflected right ascension and declination of 3C273B were fixed at the values given by Rogers et al. (1973), and the components of the Haystack-Green Bank baseline vector were fixed at the values determined by Hinteregger et al. (1972), with the small offsets between the NRAO antennas and between the Haystack and Westford antennas having been determined from a combination of conventional geodetic surveys and relevant short-baseline-interferometer observations. The rotations of the baseline vectors with respect to the inertial frame of the sources were calculated using standard formulas for precession and nutation (Her Majesty's

Nautical Almanac Office and the United States Naval Observatory, 1961), the instantaneous coordinates of the pole and UT.1 interpolated between the 10-day smoothed values published by the Bureau International de l'Heure, and formulas for the displacements due to solid-earth tides based on Table 3a in Melchior (1966). The effect of the earth's neutral atmosphere on the observable was calculated from the model of Chao (1968). A separate value of the parameter representing the zenith atmospheric delay for each end of the long baseline on each day of observation (except, as discussed below, on October 4, 10, and 11), was included as an unknown in the simultaneous least-squares solution. The relatively small effect of the daytime ionosphere on our observable was calculated from a simple model in which the electron density varied as the cosine of the local mean solar time, and in which the integrated electron content along a vertical path at noon was taken to be  $5 \times 10^{17}$  el m<sup>-2</sup>. We also modeled the average solar corona, assuming its density to vary as the inverse square of the radius from the sun, with 5,000 el cm<sup>-3</sup> at 10 r<sub>⊙</sub>.

The sensitivity of our gravitational-deflection result to the fixed value assumed for each of the parameters des-

cribing the baseline-vector components, the undeflected position of 3C273, polar motion and the variation of UT.1, solid-earth tides, the ionosphere, the neutral atmosphere, and the solar corona was investigated by repeating the simultaneous solution for  $\gamma$ , the position of 3C279, and all of the other unknown parameters with deliberate changes made to the values of these fixed parameters. We also examined the effects of possible  $2\pi$  phase-connection errors, and of omitting certain days' observations from the solution.

#### IV. Result and Estimate of Uncertainty

Our best estimate of  $\gamma$  based on all the usable observations, was 0.976. The formal standard error was 0.009, based on the root-mean-square value of  $100^\circ$  of the postfit DFP residuals and on the assumption that the observations, 3 minutes apart, had statistically independent errors. These residuals are plotted in Figure 9. It is clear that the errors are correlated over times significantly longer than 3 minutes. The perhaps more accurate assumption that every 10th point, with 30-minute spacing, was independent would have led to a formal error greater by a factor of  $\sqrt{10}$ , or approximately 0.03. But no estimate of the uncertainty which is derived entirely from the properties of postfit residuals can be trusted: the most sig-



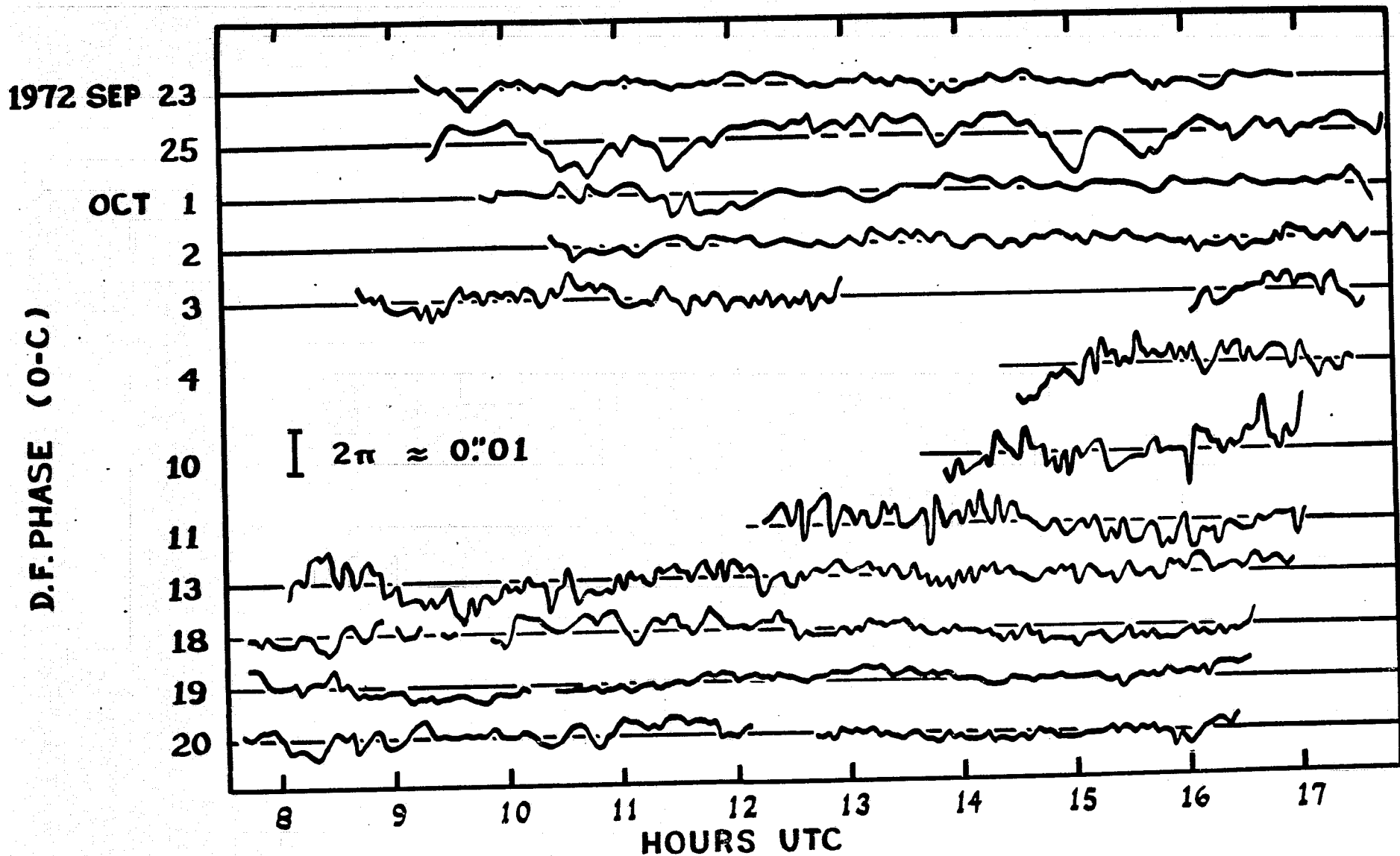


Figure 9. Postfit residuals (observed minus computed values) for the difference fringe phase. A change of  $2\pi$  in the difference fringe phase corresponds to an apparent change in relative source direction of about 10 milliarcsec, as indicated. On 29 September, the ray path to 3C273B passed within about 20 solar radii of the sun and at 9 hr UT on 8 October, 3C279 was occulted by the sun with the apparent separation increasing by about 4 solar radii per day. Coronal turbulence caused the omissions of data on parts of 3, 4, 10, and 11 October; the gaps on 18, 19, and 20 October reflect missing recordings.

nificant, long-term trends of the measurement error as a function of time may have been absorbed in the model-fitting process in such a way that they contributed to the errors of the estimated parameters, but were not revealed in the residuals. Furthermore, errors in the assumed values of fixed parameters, such as the interferometer baseline-vector components, might seriously affect the solution but have no perceptible effect on the residuals. In order to evaluate the uncertainties due to both kinds of error, we performed two kinds of computer experiments with the DFP data.

To estimate the uncertainty due to random, but slowly-varying errors of measurement, we took the DFP data from each day separately, for six days (23 September, and 1, 2, 18, 19, and 20 October) when the sun was relatively far from both radio sources, and we made independent solutions for the right-ascension difference between the sources, keeping both declinations fixed and setting  $\gamma$  equal to 1. The rms scatter of the results of these six solutions about their mean value was  $0^{\text{S}}.00025$ , whereas the formal standard errors (assuming statistical independence for 3-minute spacing of the data) averaged only  $0^{\text{S}}.00007$ . Thus, the results of this computer experiment confirm that the

originally-obtained value of the formal standard error for  $\gamma$  should be multiplied by a factor of between 3 and 4, in order to reflect the correlation of DFP measurement errors over times greater than the basic 3-minute smoothing interval.

In order to determine the contribution to the uncertainty of our estimate of  $\gamma$  due to errors in the values assumed for the parameters which were fixed in our solution, we repeated the original solution a number of times, each time changing the value of one of these parameters by no less, and often by grossly more, than our estimate of its true uncertainty. The results of these sensitivity tests are summarized in Table 4. A few of the entries in this table require explanation, as follows.

The x and y coordinates of the pole, and the difference between Universal Time (UT.1) and Atomic Time (TAI, A.1, or UTC) are interpolated in our analysis program from values tabulated at 10-day intervals, with one tabular argument corresponding to UTC 1972 October 9.0. In the tabulation of each of these three quantities we made two types of change: (i) to the October 9.0 entry alone, and (ii) to the October 9.0 and all following entries equally. Thus we considered changes which were nearly symmetrical, and

Table 4. Magnitudes of changes in the estimate of  $\gamma$  produced by changes in the values assumed for fixed parameters

<u>Parameter</u>	<u><math>\Delta</math>(parameter)</u>	<u><math> \Delta\gamma </math></u>
Both Green Bank antennas	10 m	0.00002
geocentric radius	10 m	0.00005
longitude		
One Green Bank antenna		
radius	1 m	0.00002
longitude	1 m	0.00003
3C273B		
right ascension	1"	0.0001
declination	1"	0.00005
Polar motion (see text)	1 m	0.005
Variation of UT.1 (see text)	2 ms	0.01
Earth tide amplitude at Haystack	100 %	0.007
Ionosphere electron density	100%	0.003
Solar corona mean electron density	100%	0.016
Haystack atmosphere zenith delay		
October 4	0.2 ns	0.01
October 10	0.2 ns	0.006
October 11	0.2 ns	0.003

also nearly antisymmetrical with respect to the time of the occultation of 3C279. In Table 4 we list the worst-case results, those showing the greatest effect on the estimate of  $\gamma$ . It should be noted that the estimate of  $\gamma$  is sensitive to time-variations of the errors in the pole coordinates and UT.1, but not significantly to constant errors in these quantities (errors which are equivalent to constant errors in the baseline-vector components or the source coordinates).

Atmospheric-delay parameters were fixed in our solution only for October 4, 10, and 11 -- the only days when uncertainties in the phase-connection, caused by strong solar-coronal fluctuations, prevented us from obtaining the unbroken record of the DFP over the wide range of source elevation angles which is necessary in order reliably to distinguish atmospheric effects from source-position effects on the DFP. On the remaining days of our experiment, the phase connection was sufficiently continuous that the atmospheric parameters were able to be estimated simultaneously from the DFP data. The mean values of the Haystack and the Green Bank zenith atmospheric delay parameters obtained for these other days were used to fix the corresponding parameter values on October 4, 10, and 11. What errors might

have been introduced by fixing these parameters at mean values? Our interferometric observable is sensitive primarily to the difference between the Haystack and the Green Bank atmospheric delay parameters. (Although both were normally estimated, the formal correlation between them on a given day was always approximately 0.99.) The rms scatter of the differences between the Haystack and the Green Bank values obtained on all the days other than October 4, 10, and 11 was 0.19 ns. This value provides an upper bound to the actual variation from day to day, because it includes the effects of errors in the estimates of the daily values. Therefore it seems conservative, in Table 4, to allow for changes of 0.2 ns in the atmospheric-delay parameters of October 4, 10, and 11.

If each of the fixed parameters listed in the first column of Table 4 is regarded as having a  $1-\sigma$  uncertainty equal to the corresponding entry in the second column, then the uncertainty in the estimate of  $\gamma$  due to the combination of these causes alone is given by the root-sum-of-squares of the third-column entries, or 0.024. If, conservatively, we consider the effects of errors in these parameters to be independent of those measurement errors which account for the scatter of the postfit DFP residuals

and of our six trial right-ascension solutions, we obtain a combined uncertainty of  $[(0.024)^2 + (0.035)^2]^{1/2} = 0.042$ .

Finally, we consider the possibility that, despite our elaborate precautions, one or more errors were committed in the phase-connection process, so that a spurious  $2\pi$  change was inserted into the DFP data. For several reasons, the only days on which phase-connection errors could be considered seriously are October 4 and 10, the days closest to occultation. By deliberately inserting single  $2\pi$  "errors" into the data at various times, we found that we could not alter the estimate of  $\gamma$  by as much as 0.01 except for October 4 and 10. We also found that the deletion of any single day's observations from the data set produced less than a 1-percent change in the estimate of  $\gamma$ , and a negligible change in the formal standard error, except for October 4, 10, and (in this test) the 11th. An accidental  $2\pi$  error on any day other than these three would also be rather conspicuous in the post-fit residuals.

A  $2\pi$  error deliberately introduced on October 10 produced a maximum change in  $\gamma$ , of 0.011, if the time of the insertion was near 20<sup>h</sup> UTC. On October 4 the time of maximum sensitivity to a  $2\pi$  error was also near 20<sup>h</sup> UTC, when a single  $2\pi$  error changed the estimate of  $\gamma$  by 0.09. For such an error one hour earlier or later, the sensitivity was halved, and, as expected, the sensitivity approached

zero as the error-insertion time approached the beginning or end of the observation span. If one assumes that exactly one  $2\pi$  error of either sign occurred on October 4 (on the ground that two or more errors of the same sign would be too conspicuous to go undetected), with the time of occurrence randomly distributed with uniform probability density between the beginning and end of observations, the standard deviation of the resulting error in the estimate of  $\gamma$  is 0.05.

If the observations from October 4 are deleted entirely, the solution for  $\gamma$  increases by 0.069; deleting the observations from October 10 alone changes the solution by an approximately equal and opposite amount, -0.061; deletion of the October 11 data changes the result by +0.049. The formal standard errors for these solutions, after multiplication by the square root of ten to allow for correlations of measurement errors over 30-minute intervals, were all about 0.05. If none of these days -- the only ones for which phase connection might conceivably be questionable -- are included in the fit, the solution  $\gamma = 1.031$  is obtained, greater by 0.055 than our all-inclusive result, but within one standard deviation of it. We conclude from these tests that coronal phase fluctuations on the days nearest occultation, acting both directly and indirectly through possibly-induced phase-misconnections, contribute no more than 0.04 to the  $1-\sigma$  uncertainty of the combined solution for  $\gamma$ . Combining all the sources of error listed in Table 4, as if independent,



with the coronal-fluctuation uncertainty leads to\*

$$\gamma = 0.98 \pm 0.06, \tag{4.1}$$

or, equivalently

$$\left(\frac{1+\gamma}{2}\right) = 0.99 \pm 0.03. \tag{4.2}$$

#### V. Future Experiments

Within the next few years, improved equipment and techniques will enable us to perform more accurate radio-interferometric measurements of the solar gravitational deflection than we were able to do in 1972. Based on the discussion in Section IV, we list in Table 5 all of the error sources which, in our 1972 experiment, we believe contributed more than 0.001 to the uncertainty in the estimate of  $\gamma$ . In this section, we discuss, in turn, the most promising method of reducing the uncertainty contributed by each of these sources.

---

\*The results here are rounded to only two significant figures in view of the uncertainty which affects the second decimal place.

Table 5. Principal sources of uncertainty in the 1972 VLBI determination of  $\gamma$ .

<u>Source</u>	<u>Estimated Contribution to Uncertainty in <math>\gamma</math></u>
Polar motion, UT.1, solid-earth tides	0.013
Atmosphere	0.012
Ionosphere	0.003
Mean solar corona	0.016
Inhomogeneity of solar corona, including possible " $2\pi$ " phase-connection errors	0.04
Scatter of postfit residuals (after allowance for correlations between errors)	0.035
Root-sum-of-squares of above	0.06

Polar motion, variations of UT.1, and solid-earth tides all affect the motion of the interferometer baseline vector. Their effects could be determined independently, and the uncertainty which they introduce in the determination of  $\gamma$  reduced to negligible levels, if at least three radio sources were observed in addition to the one occulted by the sun. (Our 1972 experiment involved the observation of only one other source, 3C273B, by which the effects of local-oscillator instabilities were eliminated.) The additional, baseline-calibrating, sources could be observed at night, before the near-sun sources had risen, or after they had set.

Short-term atmospheric-delay fluctuations would not increase significantly if the length of the interferometer baseline were increased up to approximately 4000 km, for example by using the Haystack Observatory and the Owens Valley Radio Observatory (OVRO). But the effect of these fluctuations in terms of equivalent source-position error would decrease in inverse proportion to the baseline length. Much beyond the 4000-km length, further increases would yield diminishing returns due to the decreased mutual visibility. Assuming that the atmospheric fluctuations were responsible for most of the scatter of the DFP residuals in 1972, except on the days nearest occultation,

we might expect a similar experiment performed with the Haystack-OVRO interferometer to yield a result for  $\gamma$  with uncertainty, due to atmospheric effects alone, of about 0.007.

Effects of atmospheric refraction could be reduced, for any baseline length, if additional sources which bracketed the position of the source occulted by the sun could also be observed nearly simultaneously. It is also possible that the atmospheric delay could be calibrated independently by passive radiometric measurements at infrared or microwave wavelengths (Schaper et al, 1970).

The ionosphere and the solar corona both affect our observable by amounts which, in terms of equivalent delay, are inversely proportional to the square of the observing frequency. The most straightforward way to reduce their effects is to observe at a higher frequency. Several antennas are available\* which are suitable for VLBI observations at 15 GHz, about twice the presently-used frequency. Connected pairs of antennas, which would enable the present four-antenna technique to be employed, are not yet equipped to operate at such high frequencies. However, difference observations could also be made by switching the pointing of a single long-baseline interferometer rapidly back and forth between the different sources if coronal phase fluctuations were sufficiently reduced by virtue of the higher operating frequency to enable phase-connection between the intermittent observations of each source, or if unambiguous

---

\*These include antennas at the Haystack Observatory, the NRAO at Green Bank, the NASA Deep Space Network in Goldstone, California, and a number of others.

group-delay observations were made (see below). Doubling the observing frequency would reduce the ionospheric contribution to the uncertainty in the estimate of  $\gamma$  to less than 0.001, and the uncertainty due to the mean\* solar-corona to about 0.004, all other aspects of the experiment remaining the same.

The equivalent source-position error associated with a  $2\pi$  phase connection error would decrease inversely if the baseline length were increased. Unfortunately, the probability of making  $2\pi$  errors in the phase-connection of observations near the sun would increase substantially, because the reduced correlation of coronal density fluctuations between the ray paths from the source to the two more widely separated antennas would result in greater, and more rapid, fringe phase fluctuations. An attempt to cope with these fluctuations

\* We distinguish here the mean effect from that due to the inhomogeneity of the corona, which causes short-term fluctuations in the fringe phase.

simply by increasing the receiving-system bandwidth or reducing the system noise temperature in order to shorten the necessary coherent-integration time might be fruitless, for two reasons. First, these improvements alone would do nothing to eliminate interruptions of the observations due to equipment and operator malfunctions, occasional defects in magnetic tapes, etc. Rapid phase-fluctuations during such interruptions would cause phase-connection errors regardless of the bandwidth or system temperature of the interferometer. Second, even if all interruptions could be eliminated, and the phase fluctuations followed correctly, the fluctuations themselves might contribute approximately the same uncertainty in the determination of  $\gamma$  for a long baseline as for a short baseline because the size of coronal fluctuations may be approximately proportional to the baseline length (Knight, 1973), all else remaining the same. We conclude that the use of a baseline much longer than that of Haystack-Green Bank might not be very advantageous unless either the observing frequency were also

increased, to reduce the phase fluctuations due to the corona, or two observing frequencies were used to allow these fluctuations to be eliminated. Even with the observing frequency kept near the present 8-GHz value, however, a marginal improvement might be gained by not observing so close to the sun. The size of the coronal fluctuations decreases approximately as the inverse square of the solar elongation, whereas the gravitational deflection decreases only as the inverse first power of the elongation.

Perhaps the simplest means to surmount the problems of phase connection is to make use of group delay measurements in any future experiment.

If the uncertainty in the determination of the group delay could be made less than the reciprocal of the (center) observing frequency, then the group-delay measurement could be used to resolve the " $2\pi$ " ambiguity in the associated fringe-phase measurement, in all observations far from the sun. The utilization of this "bootstrap" procedure would enable the full accuracy which is inherent in the use of the connected-phase observable to be achieved with only intermittent observation of a source when it is not within a few degrees of the sun. When the source is close to the sun, continuous observations which enabled the fringe phase to be followed unambiguously by itself, and which at the same time included accurate group-delay measurements, would be particularly useful because the corona introduces equal-magnitude but opposite-sign fluctuations into the group and

phase delays. Thus, accurate group-delay and phase-delay data can be combined to eliminate the effect of plasma (ionosphere as well as solar corona) on the observations. This important possibility, if realized, would make it unnecessary to go to much higher frequencies than the presently-used 8 GHz in order to achieve a major improvement in the accuracy of the experiment.

To measure the group delay at 8GHz with the requisite accuracy, error no greater than about 10 psec, will require substantial, but achievable, improvements in our instrumentation. Assuming no improvement in receiving-system temperatures ( $\sim 100^\circ\text{K}$ ) or in total spanned bandwidth of receiver front ends (now  $\sim 500$  MHz), we can calculate the recorded-bandwidth-integration-time product necessary to reduce the group-delay uncertainty to 10 psec for observations of a source with a correlated flux density of 3 Janskys. We find, for an interferometer composed of one 120-ft and one 85-ft -diameter antenna, that the signal-to-noise ratio imposes an uncertainty,  $\sigma_\phi$ , in the determination of the fringe phase of approximately

$$\sigma_\phi = 500 \cdot N^{-1/2} \text{ radians,} \quad (5.1)$$

where N is the number of bits recorded at each site and crosscorrelated for each phase measurement. (In our 1972 experiment, in which we recorded  $7.2 \times 10^5$  bits per second,



this formula predicts  $\sigma_\phi \approx 0.6$  radians for a 1-second integration, in good agreement with our experience.)

If we consider that the group delay will be determined from the fringe-phase difference between two bands 200 MHz apart, then the requirement of  $\sigma_{\Delta\tau} \approx 10$  psec leads to a requirement of  $\sigma_\phi \approx 0.009$  radians for each band, or  $N \approx 3 \times 10^9$  bits for each band. With our present recording system it would take over 2 hours to perform this measurement -- longer than we would desire. However, an improved recording system, called the Mark III, is now under development at the Haystack Observatory and promises to allow data recording rates in excess of  $10^8$  bits per second. Use of this system would enable the necessary group-delay measurement to be performed in less than 1 minute -- a very reasonable time. We note that the coherent integration of the signals in each band could be carried out for much shorter intervals, such that solar-coronal fluctuations do not destroy phase coherence, and the between-bands phase differences from the many short integrations could then be averaged for 1 minute or more in order to obtain the group delay. For example, with the Mark III system, in 0.03 second we could record  $1.5 \times 10^6$  bits for each of two 25 MHz-wide bands, obtaining a measurement of the fringe phase in each band with  $\sigma_\phi \approx 0.4$  radian, or of the between-bands phase difference with an uncertainty of 0.57 radian. The incoherent average of the 2000

independent measurements obtained in 1 minute would yield an uncertainty of  $0.57/(2000)^{1/2} \approx 0.013$  radians for the phase difference, equivalent to 10 picoseconds in group delay, as required.

We are not able to say, at present, exactly what configuration future experiments will have, because we cannot predict with certainty, for example, when antenna-receiver systems suitable for VLBI at 15 GHz and with phase-stable connections between adjacent pairs of antennas, or much lower-noise or wider-bandwidth X-band front ends, or  $10^{-8}$ -bit-per-second recorders will become available. The time scales for all of these improvements depend more on the availability of funding, than on the electronic state of the art. However, it seems very reasonable to expect that, within 5 years, a combination of such improvements will enable a VLBI determination of the solar gravitational deflection of radio waves to be made with an uncertainty

$$\sigma\left(\frac{1+\gamma}{2}\right) \lesssim 0.003.$$

References

- Bare, C. C. et al. (5 authors) 1967, *Science* 157, 189.
- Chao, C. C. 1970, Jet Propulsion Laboratory Technical Memo. 391-129.
- Counselman, C. C. et al. (11 authors) 1974, *Phys. Rev. Lett.* 33, 1621.
- Fomalont, E. B. and R. A. Sramek 1975, *Ap. J.* (in press).
- Hill, J. M. 1971, *Mon. Not. R. Astr. Soc.* 158, 7P.
- Hinteregger, H. F. et al. (9 authors) 1972, *Science* 178, 396.
- H. M. Nautical Almanac Office and U. S. Naval Observatory 1961, Explanatory Supplement to the Astronomical Ephemeris and American Ephemeris and Nautical Almanac, (H. M. Stationery Office, London).
- Knight, C. A. 1973, private communication.
- Melchior, P. 1966, The Earth Tides, (Pergamon Press, Oxford), p. 33.
- Muhleman, D. O., R. D. Ekers, and E. B. Fomalont 1970, *Phys. Rev. Lett.* 24, 1377.
- Riley, J. M. 1973, *Mon. Not. R. Astr. Soc.* 161, 11P.
- Rogers, A. E. E. 1970, *Radio Science* 5, 425.
- Rogers, A. E. E. et al. (8 authors) 1973, *Ap. J.* 185, 801.
- Schaper, L. W., D. H. Staelin, and J. W. Waters 1970, *Proc. IEEE* 58, 272.
- Seielstad, G. A., R. A. Sramek, and K. W. Weiler 1970, *Phys. Rev. Lett.* 24, 1373.
- Shapiro, I. I. 1967, *Science* 157, 806.
- Sramek, R. A. 1971, *Ap. J.* 167, L55.
- Sramek, R. A. 1973, in Experimental Gravitation, ed. B. Bertotti (Academic Press, New York).
- Weiler, K. W., R. D. Ekers, E. Raimond, and K. J. Wellington 1974, *Astron. & Astrophys.* 30, 241.